

Period doubling of spiral waves and defects

Björn Sandstede
Department of Mathematics
University of Surrey
Guildford, GU2 7XH, UK

Arnd Scheel
Department of Mathematics
University of Minnesota
Minneapolis, MN 55455, USA

August 24, 2006

Abstract

Motivated by experimental observations in the light-sensitive Belousov–Zhabotinsky reaction and subsequent numerical works, we discuss period-doubling bifurcations of spiral waves and other coherent structures. We report on explanations of the observed phenomena which involve a detailed analysis of spectra, and of the associated eigenfunctions, of defects on bounded and unbounded domains.

1 Introduction

Spiral waves arise in many biological, chemical and physical systems. They rotate rigidly as functions of time, and a typical spatial profile of a planar spiral wave is shown in Figure 1. The importance of spiral waves is partly due to the fact that experimentally observed patterns are often organized by interacting spirals. Upon varying system parameters, spiral waves may destabilize, and the resulting instabilities lead often to more complex coherent patterns or to spatio-temporally disorganized dynamics. Examples of experimentally observed instabilities are meander instabilities [14, 17, 21], core [45] and far-field breakup [23], and period-doubling instabilities [24, 43].

From a classical dynamical-systems viewpoint, we expect that the transition to complicated dynamics is initiated by a sequence of generic local or global bifurcations: Saddle-node and Hopf bifurcations in the case of equilibria, and saddle-node, Hopf and period-doubling bifurcations in the case of periodic orbits. Indeed, chemical reactions can be modelled by reaction-diffusion systems in finite domains for which bifurcations can be reduced to finite-dimensional center manifolds, and where instabilities are therefore expected to be of the aforementioned type.

In a first attempt to understand spiral-wave instabilities, we can view spirals as time-periodic solutions whilst disregarding their spatial structure: note that spirals rotate rigidly as functions of time and that their wave pattern repeats itself after one period of rotation; see Figure 1. Thus, from this viewpoint, we expect to see Hopf and period-doubling bifurcations as typical precursors on the route to complicated spatio-temporal dynamics. Hopf bifurcations have indeed been observed and give rise to meander instabilities [1]. What appears to be chaotic hypermeander of spiral tips has also been observed for parameter values far beyond the meandering transition but, to our knowledge, the question whether complicated hypermeander is actually caused by subsequent secondary bifurcations has not yet been settled.

More recently, a different type of instability has been observed both in experiments [43] and in numerical simulations [13]. The primary spiral destabilizes as illustrated in Figure 1 and gives rise to a new spiral wave that emits wave trains with doubled wavelength and temporal period. An additional feature of this transition

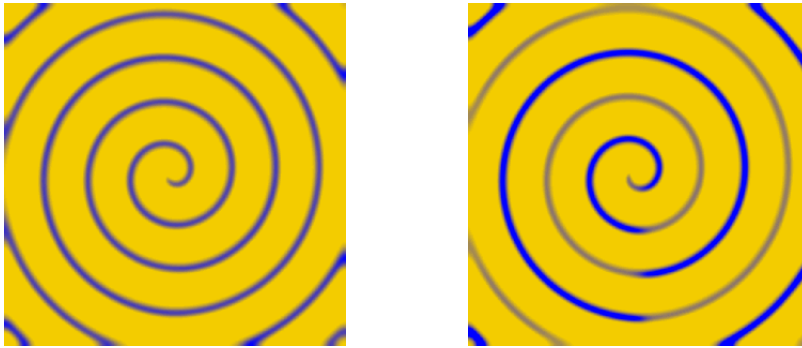


Figure 1: *Snap shots of the w -component of 2D spiral waves in the Rössler equation (1.4) are shown for two different parameter values: The left figure shows a rigidly-rotating spiral wave for $C = 2.95$ [MOVIE], while the right figure shows the spiral wave for $C = 3.4$ after a period doubling bifurcation [MOVIE]. The period-doubled spiral exhibits a line defect, which emanates from the core and ends at the bottom of the boundary, in order to accommodate the phase-shifted wave trains to either side.*

is the occurrence of a line defect that emerges from the spiral core and which accommodates the necessary mismatch of the phases of the oscillations that are emitted by the spiral core. The pattern still repeats itself but only after two rotations of the spiral core. Thus, the spiral wave, regarded as a time-periodic solution, has undergone a period-doubling bifurcation and, in accordance with the literature, we will refer to this instability as *period doubling* of spiral waves.

This apparently straightforward explanation is, however, too simple. Consider, for example, the spiral wave as a solution in a circular domain. We may then pass to a rigidly corotating coordinate frame in which the spiral wave becomes an equilibrium. In particular, we can obtain the Floquet multipliers of the spiral wave in the original laboratory frame simply by exponentiating the eigenvalues of the spiral wave in the corotating frame where the spiral is an equilibrium. An application of the spectral mapping theorem then shows that a simple eigenvalue $\rho = -1$ cannot occur for the exponential of the real linearization in the corotating frame. In other words, in rotationally symmetric domains, spiral waves are equilibria when considered in a corotating frame, which generically undergo only saddle-node or Hopf bifurcations. From this perspective, period doubling ceases to be meaningful as an instability mechanism.

Thus, the only conceivable explanation left is that the instability is a Hopf bifurcation. Since the temporal period of the bifurcating patterns observed in experiments and numerical simulations is approximately twice the period of the primary spiral, the Hopf frequency ω_H needs to be in a 2:1 resonance with the rotation frequency ω_* of the spiral wave so that

$$\omega_H = \frac{\omega_*}{2}.$$

From a genericity viewpoint, it is therefore important to understand which mechanism enforces this 2:1 resonance of the Hopf frequency of eigenvalues and the rotation frequency of the spiral wave. This natural question is indeed the central point of this paper.

The seemingly artificial choice of the corotating frame can be put in a slightly more systematic context once the symmetries of the problem are taken into account. Posing the underlying reaction-diffusion system on a circular domain, rotations in $SO(2)$ of the domain act on patterns and map solutions of the system to solutions. Spiral waves are relative equilibria with respect to this group action, that is, their time evolution is equivalent to the action of the group: Spirals are rigidly rotating. The isotropy of the spiral waves that we consider is trivial: Only a full rotation by 2π maps the spiral profile onto itself. Consequently, center manifolds near spiral waves are principal fiber bundles, given as a direct product of the underlying symmetry group $SO(2)$ and a complement of the tangent space of the group orbit in the center eigenspace [39]. In particular, the center manifold is a globally trivial bundle, which provides yet another reason for why the

case of a simple negative Floquet multiplier -1 is precluded for period-doubling bifurcations of spiral waves as this scenario requires the center manifold to be non-orientable. The structure of the principal fiber bundle can be understood by first constructing a center manifold in a Poincaré section, which is also a section to the group orbit, and then transporting the center manifold along the periodic orbit using the group action.

Symmetry is also the key to understanding the meandering patterns that arise at Hopf bifurcations. As first pointed out by Barkley [1], the meandering motion of spiral waves can be understood if we consider the spiral wave on the entire plane where, in addition to rotations, spatial translation of patterns maps solutions to solutions. The full symmetry group is therefore the special Euclidean group $SE(2)$ of translations and rotations in the plane. Center manifolds near relative equilibria can still be described as principal fiber bundles $SE(2) \times V$ where V corresponds to the Hopf eigenmodes. The dynamics on the center manifold is of skew-product form: After an appropriate reparametrization of time, the dynamics near onset are governed [6, 11, 39] by the ordinary differential equations (ODEs)

$$\begin{aligned}\dot{a} &= e^{i\varphi}[v + O(|v|^2)] \\ \dot{\varphi} &= \omega_* \\ \dot{v} &= [\mu + i\omega_H]v - (1 - i\alpha)|v|^2v\end{aligned}\tag{1.1}$$

where φ denotes the phase of the spiral, that is, its angle of rotation relative to a fixed reference frame, $a = x + iy$ is its position, and $v \in \mathbb{C}$ parametrizes a neighborhood of the origin in the Hopf eigenspace. Substituting the periodic orbit $v_*(t)$ with frequency $\omega_H + \mu\alpha$ of the v -equation and the solution $\varphi_*(t) = \omega_*t$ of the φ -equation into the equation for a , and expanding the resulting equation in Fourier modes, we find that the solution $a_*(t)$ is given by

$$a_*(t) = \sum_{k=-\infty}^{\infty} a_k \frac{e^{i[\omega_* - k(\omega_H + \mu\alpha)]t} - 1}{\omega_* - k(\omega_H + \mu\alpha)}\tag{1.2}$$

so that the spiral tip stays bounded unless ω_* and ω_H are resonant: When

$$\omega_* = \ell\omega_H \quad \text{for some } \ell \in \mathbb{Z},\tag{1.3}$$

then the tip position $a_*(t) = a_\ell t + \dots$ is unbounded near $\mu = 0$, and the spiral wave drifts with velocity a_ℓ . The resonance $\ell = 1$ has been observed frequently in experiments [1, 42].

Returning to the period-doubling instability of spiral waves, we have already inferred that period doubling ought to be a resonant Hopf bifurcation with $\ell = 2$ in (1.3). The drift predicted by (1.2) had not been observed originally in the experiments [43] or the numerical simulations [13]. Based on the theoretical predictions outlined above, we observed drift in the Rössler system

$$\begin{aligned}u_t &= 0.4 \Delta u - v - w \\ v_t &= 0.4 \Delta v + u + 0.2v \\ w_t &= 0.4 \Delta w + uw - Cw + 0.2,\end{aligned}\tag{1.4}$$

upon varying C (and report on these results in §6 below). Independently, drift was also observed in [3] for the system (1.4).

In summary, the supposition of an exact 2:1 resonance of the Hopf frequency of eigenvalues and the rotation frequency of the spiral wave leads to the prediction that period-doubled spirals should drift which was, in turn, verified in numerical simulations. Thus, the remaining key question is what enforces this resonance which seems to be non-generic and should not occur in one-parameter systems such as (1.4).

At this point, it is time to emphasize that the reduction results for planar patterns in the presence of the non-compact Euclidean group hold only for localized rotating waves. For Archimedean spirals, the presence of

essential spectrum on the imaginary axis prevents a reduction to a finite-dimensional system. While this issue may appear to be of purely technical nature for meandering instabilities where theoretical predictions are in excellent agreement with experimental and numerical results, the situation is different for period-doubling instabilities. We shall argue that period doubling of spirals is not caused by isolated point spectrum but instead by the essential spectrum of the asymptotic wave trains.

Specifically, we shall show that ordinary period-doubling bifurcations of wave trains in the travelling-wave equation create 2:1 resonances of the essential spectra of planar spiral waves that are spatially asymptotic to these wave trains in their far field. More precisely, period-doubling instabilities of wave trains manifest themselves for planar spiral waves in the form of curves of essential spectrum that cross the imaginary axis first at exactly $\Lambda = \pm i\omega_*/2$. In particular, robust 2:1 resonances can occur in an open set of one-parameter families of reaction-diffusion systems. When posed on physically relevant bounded domains such as disks of radius R , we had shown previously in [31, 37, 38] that spiral spectra accumulate in the limit $R \rightarrow \infty$ onto the so-called absolute spectrum. We show here that absolute spectra of wave trains near period-doubling bifurcations are symmetric with respect to reflections across $\text{Im } \Lambda = i\omega_*/2$: One generic possibility is therefore that the absolute spectrum lies entirely on the line $\text{Im } \Lambda = i\omega_*/2$, leading again to a 2:1 resonance. The latter case occurs, in fact, for wave trains with small wave numbers near spatially homogeneous oscillations. Lastly, we shall also investigate the nature of the line defect apparent in Figure 1.

The rest of the paper is organized as follows. We analyse spatio-temporal period doubling of one-dimensional wave trains in §2 where we also introduce background material on dispersion relations, group velocities, and absolute and essential spectra. Building upon these results, we investigate in §3 spatio-temporal period-doubling for one-dimensional sources. In §4, these results are adapted to planar Archimedean spiral waves, building on our results on spiral spectra in [31, 37, 38]. In §5, we use spatial dynamics to analyse period-doubling bifurcations near spatially homogeneous oscillations. Lastly, §6 is devoted to an application of these ideas to the Rössler system (1.4) in which period doubling had been observed previously. We conclude in §7 with a discussion of the limitations of our approach and open problems.

2 Spatio-temporal period-doubling of wave trains

Our interest in this section is to study period-doubling bifurcations of wave trains and how these manifest themselves on the spectral level in different coordinate frames. We consider reaction-diffusion systems

$$u_t = Du_{xx} + f(u; \mu), \quad x \in \mathbb{R}, \quad (2.1)$$

for $u \in \mathbb{R}^n$ and $\mu \in \mathbb{R}$, where D is a positive diagonal matrix and the nonlinearity $f : \mathbb{R}^n \times \mathbb{R} \rightarrow \mathbb{R}^n$ is smooth. We assume that (2.1) with $\mu = 0$ has a wave-train solution $u_{\text{wt}}(kx - \omega t)$ for an appropriate wave number k and temporal frequency ω , where we assume that u_{wt} is 2π -periodic in its argument so that $u_{\text{wt}}(\xi) = u_{\text{wt}}(\xi + 2\pi)$ for all ξ .

2.1 Spatial and temporal period doubling

If the wave number k vanishes, then $u(x, t) = u_{\text{wt}}(-\omega t)$ is a spatially homogeneous oscillation which satisfies the ordinary differential equation

$$u_t = f(u; \mu). \quad (2.2)$$

Period doubling of $u_{\text{wt}}(-\omega t)$ occurs when $\rho = -1$ is a temporal Floquet multiplier of the linearization of the period map associated with (2.2) about u_{wt} . The multiplier $\rho = -1$ is generically simple, and the resulting purely temporal period doubling leads to a spatially homogeneous oscillation with frequency close to $\omega/2$.

Next, assume that $k \neq 0$. In this case, we can pass from the laboratory frame x to the comoving frame $\xi = kx - \omega t$ in which (2.1) becomes

$$u_t = k^2 Du_{\xi\xi} + \omega u_{\xi} + f(u; \mu). \quad (2.3)$$

Note that $u_{\text{wt}}(\xi)$ is an equilibrium solution of (2.3) with spatial period 2π , and we focus here on steady-state bifurcations of (2.3) which are captured by the travelling-wave ODE

$$k^2 Du_{\xi\xi} + \omega u_{\xi} + f(u; \mu) = 0. \quad (2.4)$$

Spatial period doubling of the 2π -periodic orbit $u_{\text{wt}}(\xi)$ of (2.4) occurs when

$$k^2 Dv_{\xi\xi} + \omega v_{\xi} + f_u(u_{\text{wt}}(\xi); \mu)v = 0 \quad (2.5)$$

has a nonzero solution $v_{\text{pd}}(\xi)$ with $v_{\text{pd}}(\xi + 2\pi) = -v_{\text{pd}}(\xi)$ for all ξ , corresponding to a simple spatial Floquet multiplier at -1 . This bifurcation corresponds to a generic pitchfork bifurcation of (2.3) when we pose it on the spatial interval $(0, 4\pi)$ with periodic boundary conditions. The \mathbb{Z}_2 -symmetry that turns the steady-state bifurcation into a pitchfork is generated by the shift $\xi \mapsto \xi + 2\pi$ which also generates the isotropy group of the equilibrium u_{wt} of spatial period 2π when considered on the interval $(0, 4\pi)$. Lyapunov–Schmidt reduction for the nonlinear problem (2.4) on an appropriate function space of 4π -periodic function leads to a family of spatially period-doubled equilibria that bifurcate from u_{wt} . Center-manifold reduction, or Lyapunov–Schmidt reduction [16], shows that the principle of exchange of stability holds for the temporal dynamics of (2.3) on the space of 4π -periodic functions provided the cubic coefficient of the reduced equation is nonzero. In other words, the bifurcating pattern is stable as a solution to (2.3) if it exists for parameter values for which the primary pattern u_{wt} is unstable. We refer to [7] for a discussion of the multiplicity of period-doubling eigenvalues using Evans functions.

Lastly, we interpret these results in the laboratory frame. Assuming that $k \neq 0$ and $\omega \neq 0$, we consider (2.1) on the interval $(0, 4\pi/k)$ with periodic boundary conditions. Equation (2.1) generates a compact semiflow Φ_t on $H_{\text{per}}^2(0, \frac{4\pi}{k})$, and the wave train u_{wt} corresponds to a time-periodic solution with period $T = 2\pi/\omega$. We refer to eigenvalues ρ of the linearized period map $\Phi'_T(u_{\text{wt}})$ as Floquet multipliers, which turn out to be conveniently related to the spectrum of the linearization

$$\lambda v = Dk^2 v_{\xi\xi} + \omega v_{\xi} + f_u(u_{\text{wt}}(\xi); 0)v \quad (2.6)$$

of (2.3) with 4π -periodic boundary conditions about the equilibrium $u_{\text{wt}}(\xi)$. Indeed, any nontrivial solution $v(\xi)$ to the eigenvalue problem (2.6) gives a solution $w(x, \cdot)$ of the eigenvalue problem for the period map of (2.1) in the laboratory frame via

$$w(x, t) = e^{\lambda t} v(kx - \omega t), \quad w(x, T) = e^{\lambda T} v(kx - 2\pi)$$

and vice versa. Spatial period doubling of (2.6) corresponds to $\lambda = 0$ and $v(\xi)$ with $v(\xi + 2\pi) = -v(\xi)$ for all ξ . The resulting solution $w(x, t)$ satisfies $w(x, T) = -w(x, 0)$, and therefore gives a simple Floquet multiplier $\rho = -1$. We refer to the occurrence of a simple Floquet multiplier $\rho = -1$ of $\Phi'_T(u_{\text{wt}})$ as spatio-temporal period doubling.

2.2 Essential spectra of wave trains

More generally, we can consider the linearization on the real line $x \in \mathbb{R}$. First, consider the linearization

$$v_t = Dk^2 v_{\xi\xi} + \omega v_{\xi} + f_u(u_{\text{wt}}(\xi); 0)v, \quad \xi \in \mathbb{R} \quad (2.7)$$

in the comoving frame together with the associated eigenvalue problem

$$\lambda v = Dk^2 v_{\xi\xi} + \omega v_{\xi} + f_u(u_{\text{wt}}(\xi); 0)v, \quad \xi \in \mathbb{R}. \quad (2.8)$$

We write this equation as the first-order system

$$\mathbf{v}_x = \begin{pmatrix} 0 & 1 \\ k^{-2}D^{-1}[\lambda - f_u(u_{\text{wt}}(\xi); 0)] & \omega k^{-2}D^{-1} \end{pmatrix} \mathbf{v} \quad (2.9)$$

and denote the associated 2π -period map by $\Psi_{2\pi}(\lambda)$. Spatial Floquet exponents ν/k of (2.8) or (2.9) are determined as roots of the Wronskian

$$d(\lambda, \nu) := \det \left[e^{2\pi\nu/k} - \Psi_{2\pi}(\lambda) \right]. \quad (2.10)$$

The Wronskian $d(\lambda, \nu)$ satisfies

$$\begin{aligned} \overline{d(\lambda, \nu)} &= d(\bar{\lambda}, \bar{\nu}) && \text{complex conjugation} \\ d(\lambda, \nu) &= d(\lambda, \nu + ik\ell) && \text{artificial Floquet conjugation} \end{aligned} \quad (2.11)$$

for all integers ℓ . Spatial Floquet exponents can also be found by seeking nontrivial solutions to (2.8) of the form

$$v(\xi) = e^{\nu\xi/k} v_0(\xi), \quad v_0(\xi + 2\pi) = v_0(\xi) \quad \forall \xi \quad (2.12)$$

where v_0 is a 2π -periodic solution of

$$\lambda v = D(k\partial_{\xi} + \nu)^2 v + \frac{\omega}{k}(k\partial_{\xi} + \nu)v + f_u(u_{\text{wt}}(\xi); 0)v. \quad (2.13)$$

Purely imaginary spatial Floquet exponents $\nu \in i\mathbb{R}$ give eigenvalues λ of (2.8), and each eigenfunction (2.12) leads to a solution

$$v(\xi, t) = e^{\lambda t} e^{\nu\xi/k} v_0(\xi) \quad (2.14)$$

of (2.7). We record that spatial period doubling as discussed in §2.1 is equivalent to having a nontrivial solution v of (2.13) for $\lambda = 0$ and $\nu = ik/2$.

In the laboratory frame, the relevant linearization is

$$u_t = Du_{xx} + f_u(u_{\text{wt}}(kx - \omega t); 0)u, \quad x \in \mathbb{R}. \quad (2.15)$$

Temporal Floquet multipliers ρ and the associated Floquet exponents Λ in the laboratory frame are determined by bounded nontrivial solutions $u(x, t)$ of (2.15) with

$$u(x, T) = \rho u(x, 0) = e^{\Lambda T} u(x, 0)$$

where $T = 2\pi/\omega$. It turns out that Λ is a temporal Floquet exponent if, and only if, there is a nontrivial solution of (2.15) of the form

$$u(x, t) = e^{\Lambda t} e^{\nu x} u_0(kx - \omega t)$$

with $\nu \in i\mathbb{R}$, where u_0 is 2π -periodic in its argument. Solutions of this form for arbitrary $\nu \in \mathbb{C}$ are in one-to-one correspondence with the solutions (2.12) of (2.8) via

$$u(x, t) = e^{\lambda t} e^{\nu\xi/k} v_0(\xi) = e^{[\lambda - \nu\omega/k]t} e^{\nu x} v_0(kx - \omega t) = e^{\Lambda t} e^{\nu x} v_0(kx - \omega t)$$

with

$$\Lambda = \lambda - \frac{\omega\nu}{k} = \lambda - c_p\nu \quad (2.16)$$

where $c_p = \omega/k$ is the phase speed of the wave train u_{wt} . Thus, the temporal Floquet exponents Λ in the laboratory frame are roots of

$$\mathcal{D}(\Lambda, \nu) := d(\Lambda + c_p\nu, \nu). \quad (2.17)$$

Using (2.11), we see that \mathcal{D} satisfies

$$\begin{aligned}\overline{\mathcal{D}(\Lambda, \nu)} &= \mathcal{D}(\bar{\Lambda}, \bar{\nu}) && \text{complex conjugation} \\ \mathcal{D}(\Lambda, \nu) &= \mathcal{D}(\Lambda - i\omega\ell, \nu + ik\ell) && \text{Floquet conjugation}\end{aligned}\tag{2.18}$$

for all integers ℓ . Typically, solutions of $d(\lambda, \nu) = 0$ come in curves $\lambda = \lambda_*(\nu)$, yielding also $\Lambda = \Lambda_*(\nu)$. For $\nu \in i\mathbb{R}$, we refer to these curves as dispersion curves in the comoving and the laboratory frame, respectively. We say that a dispersion curve $\Lambda_*(\nu)$ is simple if

$$\partial_\Lambda \mathcal{D}(\Lambda, \nu) = \partial_\lambda d(\lambda, \nu) \neq 0$$

at $\Lambda = \Lambda_*(\nu)$ or $\lambda = \lambda_*(\nu)$. The derivative

$$c_g := -\frac{d \operatorname{Im} \Lambda}{d \operatorname{Im} \nu}$$

is commonly referred to as the *group velocity* in the laboratory frame. The relation (2.16) can therefore be viewed as transforming the group velocity from the laboratory to the comoving frame by subtracting the speed of the frame.

Equation (2.16) implies that spatial period doubling with $\lambda = 0$ and $\nu = ik/2$ in the comoving frame becomes spatio-temporal period doubling with $\Lambda = -i\omega/2$ and $\nu = ik/2$ in the laboratory frame. The observation that the composition of the two symmetries in (2.18) fixes $\operatorname{Im} \Lambda = -i\omega/2$ leads us to the following lemma on robustness of period doubling.

Lemma 2.1 (Robustness of spatio-temporal period doubling) *Assume that there is a simple dispersion curve $\Lambda(\nu)$ with*

$$\operatorname{Im} \Lambda(ik/2) = -\frac{i\omega}{2},\tag{2.19}$$

then the dispersion curve is reflection symmetric about the line $\operatorname{Im} \Lambda = -i\omega/2$ for ν close to $ik/2$. Moreover, (2.19) is robust under sufficiently small perturbations of the parameter value μ and the coefficients $u_{\text{wt}}(\xi)$ in (2.6).

Proof. From (2.18), we conclude that $\mathcal{D}(\Lambda, \nu) = 0$ if, and only if, $\mathcal{D}(\bar{\Lambda} - i\omega, \bar{\nu} + ik) = 0$. Upon substituting $\Lambda = -i\omega/2 + l$ and $\nu = ik/2 + i\gamma$ with $\gamma \in \mathbb{R}$ into these identities, we see that $\mathcal{D}(-i\omega/2 + l, ik/2 + i\gamma) = 0$ if, and only if, $\mathcal{D}(-i\omega/2 + \bar{l}, ik/2 - i\gamma) = 0$. Applying the implicit function theorem to both equations, and using uniqueness of solutions, we conclude that $l(-\gamma) = \bar{l}(\gamma)$ for all γ close to zero, which implies the asserted symmetry of the dispersion curve about the line $\operatorname{Im} \Lambda = -i\omega/2$. Robustness with respect to parameter variations is again a consequence of the implicit function theorem. \blacksquare

In preparation for the analysis in the following two sections, we examine the linearization in exponentially weighted spaces

$$L_\eta^2 := \{u \in L_{\text{loc}}^2; |u|_{L_\eta^2} < \infty\}, \quad |u|_{L_\eta^2}^2 := \int_{\mathbb{R}} |u(x)|^2 e^{-2\eta x} dx.\tag{2.20}$$

The spectra in L_η^2 can be computed in the same way as for $\eta = 0$ by solving (2.13) with $\nu \in \eta + i\mathbb{R}$, which yields an η -dependent family of dispersion curves $\Lambda(\nu)$ with $\operatorname{Re} \nu = \eta$. The real part of these curves depends on η according to

$$\frac{d \operatorname{Re} \Lambda}{d\eta} = \frac{d \operatorname{Re} \Lambda}{d \operatorname{Re} \nu} = \frac{d \operatorname{Im} \Lambda}{d \operatorname{Im} \nu} = -c_g,\tag{2.21}$$

where we used the Cauchy–Riemann equations for the complex analytic function $\Lambda(\nu)$ in the second equality. In particular, if the group velocity c_g is positive, then positive weight rates $\eta > 0$, which predominantly measure mass accumulating at $x \rightarrow -\infty$, push dispersion curves $\Lambda(\nu)$ towards the stable direction since $\frac{d \operatorname{Re} \Lambda}{d\eta} < 0$. This can in fact be viewed as a justification of the terminology for c_g in the sense that the group velocity measures transport from negative to positive x .

From now on, we shall always denote the temporal Floquet exponents of wave trains in the comoving frame by λ and in the laboratory frame by Λ .

2.3 Absolute spectra of wave trains

When we pass to large bounded domains with separated boundary conditions, exponential weights generate equivalent topologies for each finite domain size L . In [30], we showed that the spectrum of the linearized period map, considered on large but finite domains with typical separated boundary conditions, converges in the limit of infinite domain size. We proved that this limit is given generically by the absolute spectrum which can be computed using only the Wronskian $\mathcal{D}(\Lambda, \nu)$ and which typically consists of a locally finite collection of semi-algebraic curves.

Since the absolute spectrum is related to separated boundary conditions, it depends crucially on the frame in which the boundary conditions are imposed. As we are primarily interested in 1D sources and 2D spiral waves for which only the laboratory frame is relevant, we shall compute the absolute spectrum of wave trains in this frame. To define absolute spectra in the laboratory frame, we fix a point $\Lambda \in \mathbb{C}$ and collect all roots ν of the Wronskian $\mathcal{D}(\Lambda, \nu)$ subject to $0 \leq \text{Im } \nu < k$. As shown in [34, §3.4], these roots form a countable set $\{\nu_j\}_{j \in \mathbb{Z}}$ which depends on the choice of $\Lambda \in \mathbb{C}$. Taking the restriction on the imaginary part of the ν_j into account, we conclude from [20] that there are only finitely many roots ν_j , counted with multiplicity as solutions to an analytic equation, in any bounded region of the complex plane. Furthermore, [34, §3.4] implies that there are infinitely many roots with negative real parts and infinitely many roots with positive real part. We may therefore order the roots ν_j , repeated with multiplicity, according to their real part

$$\dots \leq \text{Re } \nu_{-k} \leq \text{Re } \nu_{-k+1} \leq \dots \leq \text{Re } \nu_{-1} \leq \text{Re } \nu_0 \leq \text{Re } \nu_1 \leq \dots \leq \text{Re } \nu_k \leq \text{Re } \nu_{k+1} \leq \dots \quad (2.22)$$

which gives a well defined labelling up to shifts in the indices and up to the ambiguity of labelling roots with equal real part. For $\text{Re } \Lambda \gg 1$, each ν_j has nonzero real part since the essential spectrum would otherwise extend arbitrarily far to the right in the complex plane. We may therefore choose the labelling in (2.22) so that $\text{Re } \nu_0 < 0 < \text{Re } \nu_1$ for $\text{Re } \Lambda \gg 1$. We then define the *absolute spectrum* in the laboratory frame as the set

$$\Sigma_{\text{abs}} = \{\Lambda \in \mathbb{C}; \text{Re } \nu_0 = \text{Re } \nu_1\}. \quad (2.23)$$

We say that the absolute spectrum is *simple* if $\text{Re } \nu_{-1} < \text{Re } \nu_{0,1} < \text{Re } \nu_2$ and call points where $\nu_0 = \nu_1$ *edges* of the absolute spectrum. Edges in simple absolute spectrum are called simple edges, and it is straightforward to see that a unique curve of absolute spectrum emerges from each simple edge. More generally, the absolute spectrum comes in curves, being defined by a single real condition for the complex parameter Λ , and we may naturally parametrize these curves using the parameter

$$s = (\text{Im } \nu_1 - \text{Im } \nu_0)^2$$

so that edges correspond to $s = 0$.

Inspecting (2.23) shows that the absolute spectrum also respects the symmetries (2.18) of the essential spectrum, namely complex conjugation and the artificial Floquet covering symmetry $\Lambda \mapsto \Lambda + i\omega$. In particular, we have the following analogue of Lemma 2.1.

Lemma 2.2 (Robustness of absolute spatio-temporal period doubling) *Suppose that a simple edge of the absolute spectrum $\Lambda(0)$ is located at $\text{Im } \Lambda(0) = -\omega/2$ for $\text{Im } \nu_0 = k/2$, then the unique dispersion curve emanating from $\Lambda(0)$ is horizontal, that is, $\text{Im } \Lambda(s) = -\omega/2$ for $s \approx 0$. Moreover, the same conclusion holds for sufficiently small perturbations of the parameter value μ and the coefficients $u_{\text{wt}}(\xi)$ in (2.6). In particular, the absolute spectrum crosses at the sharp resonance $-\omega/2$ for an open subset of one-parameter families of reaction-diffusion systems.*

Proof. The proof is similar to the proof of Lemma 2.1 and will be omitted. ■

We emphasize that the crossing of the essential spectrum at $\pm i\omega/2$ does not necessarily enforce the absolute spectrum to cross at resonance. The other generic possibility is that the absolute spectrum consists locally of two curves which are symmetric about $\text{Im } \Lambda = \pm\omega/2$ but do not contain any points with $\text{Im } \Lambda = \pm\omega/2$.

2.4 Spatially homogeneous oscillations

We show here that the hypotheses stated in Lemma 2.1 and 2.2 are met for wave trains with small wave numbers that accompany spatially homogeneous oscillations. Indeed, assume that (2.2) admits a solution $u_{\text{wt}}(-\omega t)$ which undergoes a generic temporal period-doubling bifurcation at $\mu = 0$. Moreover, assume that the Floquet spectrum of the linearized period map $\Phi'_T(u_{\text{wt}})$ of (2.1) is contained in the open left half-plane except for simple edges at $\Lambda = 0$, $\Lambda = \pm i\omega/2$ and their Floquet conjugates (note that the absolute and essential spectra of homogeneous oscillations coincide since these waves are invariant under the spatial reflections $x \mapsto -x$).

Lemma 2.3 *Under the assumptions stated above, there exists a family of wave trains, parametrized by their wave number k with $k \approx 0$, each of which undergoes a spatio-temporal period doubling which satisfies the hypotheses of Lemma 2.1 and 2.2.*

We remark that the statement of the preceding lemma will be further extended in §5.

Proof. The existence problem and the eigenvalue problem of wave trains with wave number $k = \varepsilon \approx 0$ yield the singularly perturbed boundary-value problems

$$\varepsilon^2 D\partial_\xi^2 u + \omega\partial_\xi u + f(u) = 0, \quad D(\varepsilon\partial_\xi + \nu)^2 v + \omega(\partial_\xi + \nu/\varepsilon)v + f'(u)v = \lambda v,$$

respectively, with 2π -periodic boundary conditions in $\xi = \varepsilon x$. The eigenvalue problem can be rewritten in the form

$$D(\varepsilon\partial_\xi + \nu)^2 v + \omega\partial_\xi v + f'(u)v = \Lambda v,$$

using the definition (2.16) of Λ . Writing these second-order equations as first-order equations and reducing the dynamics to a slow manifold using geometric singular perturbation theory as in [34, §3.3] shows that bounded solutions lie on the slow manifold and that the evolution on the slow manifold is obtained to leading order by formally setting $\varepsilon = 0$ in the system above. The reduced system therefore consists of a regular perturbation of a generic period-doubling bifurcation with simple Floquet multiplier which proves the claim about existence. The spectral problem with simple edges at $\Lambda = 0$ and $\Lambda = -i\omega/2$ for $\nu = 0$ and $\nu = ik/2$, respectively, is robust as well and yields the same spectral picture for $\varepsilon \approx 0$ with a possible offset in the real part of the period-doubling eigenvalue. ■

3 Period doubling of sources in one space dimension

Two-dimensional spirals are defects in the sense that, far away from the location of the spiral tip, the medium resembles locally the essentially one-dimensional planar wave trains that we encountered in the previous section. An additional property of two-dimensional spirals is the active emission of wave trains in the sense that the group velocity of the planar wave trains that are observed in the far field points in the radial direction away from the center of the spiral.

Sources are 1D analogues of spiral waves, and we discuss in this section the 1D analogue, see Figure 2, of the period-doubling instability of 2D spiral waves. We are particularly interested in investigating whether Floquet multipliers cross exactly at $\rho = -1$ or only nearby.

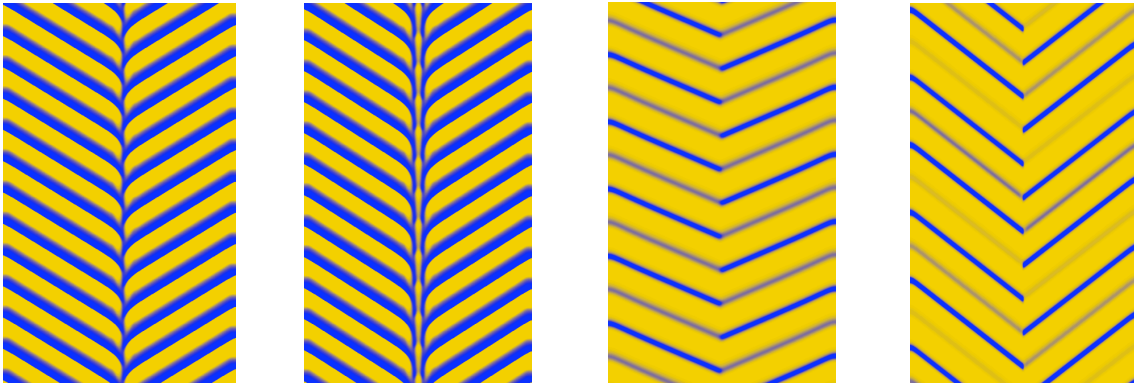


Figure 2: *From left to right: Plotted are space-time plots (time upwards, space horizontal) of 1d-spirals and 1d-targets of the Brusselator with parameters as in [34, Appendix B], and 1d-spirals and moving period-doubled sources of the Rössler system (6.1) with $C = 3.0$ and $C = 4.2$, respectively.*

3.1 Sources

Recall the reaction-diffusion system

$$u_t = Du_{xx} + f(u; \mu), \quad x \in \mathbb{R}. \quad (3.1)$$

Standing sources $u_*(x, t)$ are time-periodic solutions of (3.1) which converge to wave trains u_{wt}^\pm in the far field as $x \rightarrow \pm\infty$ whose group velocities c_{g}^\pm , computed in the laboratory frame, point away from the interface so that $c_{\text{g}}^- < 0$ and $c_{\text{g}}^+ > 0$. More precisely, we have

$$u_*(x, t) = u_*(x, t + T), \quad |u_*(x, t) - u_{\text{wt}}^\pm(k_\pm x - \omega_\pm t - \theta_\pm; k_\pm)| \rightarrow 0 \quad \text{as } x \rightarrow \pm\infty \quad (3.2)$$

where $u_{\text{wt}}(\xi; k)$ denotes a family of wave trains which are 2π -periodic in the argument ξ with temporal frequencies ω_\pm , spatial wave numbers k_\pm and phase corrections θ_\pm at $\pm\infty$, respectively. Characteristic for sources is the requirement that the group velocities, computed in the laboratory frame, are directed away from the defect so that $c_{\text{g}}^- < 0$ and $c_{\text{g}}^+ > 0$. As before, we let $\omega = 2\pi/T$ denote the temporal frequency of the source. We showed in [34] that sources occur for open, nonempty classes of reaction-diffusion systems and generically for discrete sets of asymptotic wave numbers k_\pm .

We focus here exclusively on 1d-targets and 1d-spirals which are standing sources that are reflectionally symmetric so that

$$u_*(x, t) = u_*(-x, t) \quad (\text{1d-target}) \quad \text{or} \quad u_*(x, t) = u_*(-x, t + T/2) \quad (\text{1d-spiral}) \quad (3.3)$$

for all (x, t) . Thus, 1d-target patterns are even in x for each t , while 1d-spirals are invariant when simultaneously reflecting the pattern and shifting in time by half the temporal period; see Figure 2. Reflectional symmetry implies in both cases that $k_+ = -k_- \neq 0$.

3.2 Spectra of sources on \mathbb{R}

Dynamic properties such as robustness, stability and interaction with other defects are largely determined by spectral properties of the linearization Φ'_T of the time- T map of (3.1) about the defect. Throughout this section, we will switch forth and back between Floquet exponents Λ and Floquet multipliers $\rho = e^{\Lambda T}$ in the spectrum of Φ'_T . We distinguish between the *point spectrum*, which consists of all $\rho \in \mathbb{C}$ for which $\Phi'_T - \rho$ is not invertible but still Fredholm of index zero, and the *essential spectrum*, which is the complement of the point spectrum in the spectrum. We showed in [34] that the Fredholm index of Φ'_T jumps precisely at the

dispersion curves of the asymptotic one-dimensional wave trains, computed in the frame of the defect. In particular, the essential spectrum of sources inherits the symmetry properties of the essential spectrum of the one-dimensional wave trains.

Corollary 3.1 (Robust period-doubling of sources) *There exists an open class of one-parameter families of reaction-diffusion systems where the spectrum of the linearization crosses the imaginary axis first at $\Lambda = \pm i\omega/2$.*

The multiplicity of the essential spectrum depends on whether the underlying source is reversible in the sense of (3.3) or not: Since the asymptotic wave trains at $x = \pm\infty$ of 1d-targets and 1d-spirals are related by reflection symmetry, the essential spectra of both wave trains cross the imaginary axis simultaneously. Thus, the essential spectrum of reversible sources has geometric multiplicity two, which has implications for the actual bifurcation scenario which we will discuss in §3.4.

We now discuss point spectrum. There are no structural reasons that prevent 1d-targets from having a simple point Floquet multiplier at $\rho = -1$ that crosses the imaginary axis, thus leading to a generic period-doubling bifurcation of time-periodic solutions of (3.1). Since 1d-targets are symmetric under the spatial reflections defined by

$$(\mathcal{R}u)(x) := u(-x),$$

the linearized period map leaves the spaces $\text{Fix}(\mathcal{R})$ and $\text{Fix}(-\mathcal{R})$ of even and odd functions invariant [12]. The eigenfunction belonging to a simple multiplier $\rho = -1$ is therefore either even or odd: the bifurcating sources are 1d-targets in the first case and 1d-spirals in the second case, and they have approximately twice the temporal period in both cases.

Floquet multipliers of 1d-spirals at $\rho = -1$ must, however, have geometric multiplicity two since the linearized period-T map $\Phi'_T(u_*)$ can be written as a square: Indeed, $\Phi_t(u)$ is equivariant with respect to the spatial reflection \mathcal{R} so that $\Phi_t(\mathcal{R}u) = \mathcal{R}\Phi_t(u)$ and therefore $\Phi'_{T/2}(\mathcal{R}u) = \mathcal{R}\Phi'_{T/2}(u)\mathcal{R}$. Using that $\Phi_{T/2}(u_*) = \mathcal{R}u_*$ for the 1d-spiral u_* , we obtain

$$\Phi'_T(u_*) = \Phi'_{T/2}(\Phi_{T/2}(u_*))\Phi'_{T/2}(u_*) = \mathcal{R}\Phi'_{T/2}(u_*)\mathcal{R}\Phi'_{T/2}(u_*) = [\mathcal{R}\Phi'_{T/2}(u_*)]^2.$$

We first focus on the center subspace associated with critical point spectrum of $\mathcal{R}\Phi'_{T/2}(u_*)$. Clearly this subspace is invariant under $\Phi'_T(u_*)$. An eigenvalue -1 of $\Phi'_T(u_*)$ can only be generated by eigenvalues $\pm i$ of $\mathcal{R}\Phi'_{T/2}(u_*)$ which come necessarily in complex conjugated pairs so that the eigenvalue -1 cannot be simple. If the essential spectrum of $\mathcal{R}\Phi'_{T/2}(u_*)$ is bounded away from $\pm i$, then the essential spectrum of $\Phi'_T(u_*)$ is bounded away from -1 by Fredholm algebra properties, and the spectral projection P belonging to eigenvalues near -1 can be obtained by factoring

$$\Phi'_T(u_*) - \rho = [\mathcal{R}\Phi'_{T/2}(u_*) - \sqrt{\rho}] [\mathcal{R}\Phi'_{T/2}(u_*) + \sqrt{\rho}]$$

for ρ on a small circle Γ around -1 , and computing

$$\begin{aligned} P &= \int_{\Gamma} [\rho - \Phi'_T(u_*)]^{-1} d\rho \\ &= \int_{\Gamma} [\mathcal{R}\Phi'_{T/2}(u_*) - \sqrt{\rho}]^{-1} [\mathcal{R}\Phi'_{T/2}(u_*) + \sqrt{\rho}]^{-1} d\rho \\ &= \int_{\sqrt{\Gamma}} \left([\mathcal{R}\Phi'_{T/2}(u_*) - \sqrt{\rho}]^{-1} - [\mathcal{R}\Phi'_{T/2}(u_*) + \sqrt{\rho}]^{-1} \right) d\sqrt{\rho}. \end{aligned}$$

In particular, the spectral projection of $\Phi_T(u_*)$ associated with $\rho = -1$ is given by the sums of the spectral projections of $\mathcal{R}\Phi'_{T/2}$ associated with $\rho = \pm i$. This shows that classical period doubling in the form of a simple Floquet multiplier at -1 in the point spectrum cannot occur for 1d-spirals.

Remark 3.2 *The preceding analysis also shows that the double Floquet multiplier at $\rho = -1$ for 1d-spirals will generically split into two non-real, complex conjugate multipliers since there is no structural reason which prevents the eigenvalues $\pm i$ of $\mathcal{R}\Phi'_{T/2}(u_*)$ from moving off the imaginary axis, thus moving the multipliers of the square $\Phi'_T(u_*)$ off the negative real axis.*

In preparation for the discussion in §3.3, we collect some properties of the spectra of symmetric sources in the exponentially weighted spaces

$$\hat{L}_\eta^2 := \{u \in L^2_{\text{loc}}; |u|_{\hat{L}_\eta^2} < \infty\}, \quad |u|_{\hat{L}_\eta^2} := \int_{\mathbb{R}} |u(x)|^2 e^{-2\eta|x|} dx. \quad (3.4)$$

The essential spectrum of the linearized period-T map of a symmetric source (3.3) on the space \hat{L}_η^2 is determined by the dispersion curves of the asymptotic wave trains in the spaces L^2_η from (2.20). Exploiting that the wave trains $u_{\text{wt}}^\pm(x; k_\pm)$ are related by symmetry,

$$u_{\text{wt}}^+(x; k_+) = u_{\text{wt}}^-(-x; k_-), \quad k_+ = -k_-,$$

it follows that the spatial Floquet exponents $\nu_j^\pm(\Lambda)$ that appear in the definition (2.23) of the absolute spectra of wave trains are related via

$$\nu_j^+(\Lambda) = -\nu_{1-j}^-(\Lambda) \quad \forall j. \quad (3.5)$$

In particular, we have $\nu_0^+(\Lambda) = -\nu_1^-(\Lambda)$ and $\nu_1^+(\Lambda) = -\nu_0^-(\Lambda)$ so that the absolute spectra of the asymptotic wave trains coincide and so that, for each $\Lambda \notin \Sigma_{\text{abs}}$, we can find a weight η with $\nu_0^+ < \eta < \nu_1^+$ such that the linearized period map $\Phi'_T(u_*) - e^{\Lambda T}$ is Fredholm with index zero in \hat{L}_η^2 . Note also that we can choose the weight η to be constant locally in Λ . We define the *extended point spectrum* to be the set of $\Lambda \notin \Sigma_{\text{abs}}$ such that the linearized period map is not invertible in the space \hat{L}_η^2 with η chosen as described above. We can then also define geometric and algebraic multiplicities for elements of the extended point spectrum.

3.3 Spectra of sources on finite intervals

The resonant crossing of essential spectra of sources provides some evidence for why period doubling can occur in a robust fashion. Experiments and numerical simulations are, however, posed on large but finite domains, typically with separated boundary conditions. The linearized period map on bounded domains is a compact operator, and the essential Floquet spectrum therefore empty: Instead, the absolute spectra of the asymptotic wave trains become relevant. For simplicity, we restrict ourselves to Neumann boundary conditions, thus considering

$$\begin{aligned} u_t &= Du_{xx} + f(u; \mu), & x \in (-L, L) \\ 0 &= u_x(\pm L, t), \end{aligned} \quad (3.6)$$

which are realistic for the experimental setup and which are also a standard choice for numerical simulations.

We shall focus exclusively on 1d-targets and 1d-spirals. We assume that there exists a symmetric source u_{so} such that $\Lambda = 0$ belongs to the extended point spectrum with algebraic and geometric multiplicity two. We showed in [34] that this assumption is satisfied for an open and nonempty set of reaction-diffusion systems and called this type of source elementary. To describe the influence of the boundary, we need an assumption on the boundary layer between wave trains and the boundary. We assume that (3.1) admits a *symmetric sink* u_{si} , that is, a solution of the form (3.2) which is even in x , with asymptotic wave numbers $k_{\text{si}}^\pm := k_{\text{so}}^\mp$. In particular, the group velocities of the sink point towards the center of the sink. We assume that $\Lambda = 0$ does

not belong to either the absolute or the extended point spectrum of the linearization $\Phi'_T(u_{\text{si}})$ of the period map. Again, this assumption is robust [34]. Since the sink is even, it gives solutions u_{si}^\pm of the system

$$\begin{aligned} u_t &= Du_{xx} + f(u; \mu), & x \in \mathbb{R}^\pm \\ 0 &= u_x(0, t) \end{aligned} \tag{3.7}$$

on the half-spaces \mathbb{R}^+ and \mathbb{R}^- which satisfy Neumann boundary conditions at $x = 0$, and we refer to these two solutions on \mathbb{R}^+ and \mathbb{R}^- as *boundary sinks* [34]. In this setup, we proved the following result on the existence and spectral properties of solutions on large bounded intervals.

Theorem 1 ([34, §6.8]) *Under the above assumptions, the reaction-diffusion system (3.6) has, for each $L \gg 1$, a unique time-periodic solution $u_*(x, t; L)$ which is close to the symmetric source u_{so} on $(-L/2, L/2)$ and to the appropriately translated boundary sinks u_{si}^+ and u_{si}^- on $(-L, -L/2)$ and $(L/2, L)$, respectively.*

The assumption on the existence of a symmetric sink can be verified in the special case of nearly homogeneous oscillations (see also §5.4). Recall that a homogeneous oscillation with a simple Floquet exponent $\Lambda = 0$ is accompanied by a family of wave trains $u_{\text{wt}}(kx - \omega(k)t)$ for small wave numbers $k \approx 0$.

Theorem 2 ([5]) *Assume that there is a spatially homogeneous oscillation $u_{\text{wt}}(-\omega(0)t)$ such that the Floquet multiplier $\Lambda = 0$ is a simple edge. For each $k \approx 0$, there exists a unique symmetric sink which is spatially asymptotic to the wave trains $u_{\text{wt}}(\pm kx - \omega(\pm k)t)$ at $x = \pm\infty$.*

Next, we investigate the spectrum of the linearized period map near the truncated sources that we described in Theorem 1. An outline of the proof of the following theorem will be given in Appendix A.

Theorem 3 *Assume that the extended point spectrum of the sources u_{so} on \mathbb{R} is discrete, then the spectrum of the period map of the truncated sources described in Theorem 1 converges locally uniformly in the symmetric Hausdorff distance to the disjoint union of the absolute spectrum Σ_{abs} of the wave trains u_{wt} , computed in the laboratory frame, and a discrete set of isolated points.*

The convergence towards the absolute spectrum is algebraic of order $O(1/L)$, and the number of eigenvalues in any small neighborhood of any element of the absolute spectrum converges to infinity as $L \rightarrow \infty$. The discrete part of the limiting spectrum is the union of the extended point spectrum of the source u_{so} on \mathbb{R} and the extended point spectra of the two symmetric boundary sinks u_{si}^\pm on \mathbb{R}^\pm with Neumann boundary conditions. The convergence towards the discrete part is exponential in L , and the multiplicity of eigenvalues in any small neighborhood of the discrete part is finite and stabilizes as $L \rightarrow \infty$.

We remark that the absolute spectrum is close to the essential spectrum if the wave number of the asymptotic wave trains is sufficiently close to zero; see Lemma 2.3 and also §5 below. We now discuss the implications of Theorem 3 for period doubling of symmetric sources of (3.6).

We begin with 1d-targets. Floquet exponents $\rho = -1$ in the Floquet point spectrum of a 1d-target u_{so} on \mathbb{R} will generically have multiplicity one and therefore persist as a simple multiplier $\rho \in \mathbb{R}^-$ near -1 for (3.6), with the eigenfunction lying again in the space of even or odd functions. Next, assume that the boundary sink u_{si}^+ on \mathbb{R}^- with Neumann conditions has a simple Floquet multiplier $\rho = -1$ in its point spectrum. Since the sinks u_{si}^+ and u_{si}^- are related by reflection $x \mapsto -x$, the reflected sink u_{si}^- also has a simple Floquet multiplier $\rho = -1$, and Theorem 3 shows that the truncated source u_* has two Floquet multipliers near $\rho = -1$. Since 1d-targets are symmetric under spatial reflections, the linearized period map leaves the spaces of even and odd functions invariant. The Floquet eigenfunctions of the boundary sinks on \mathbb{R}^\pm yield one even and one odd eigenfunction of the truncated 1d-target of (3.6), which can be seen via transversality arguments

in a spatial-dynamics formulation of the eigenvalue problem. In particular, the two Floquet multipliers of the persisting source on the bounded interval are both real and close to -1 but may split on the negative real line. Thus, two period-doubling bifurcations will take place, both with multipliers at $\rho = -1$, one with an even and the other one with an odd eigenfunction. In summary, period doubling of 1d-targets for (3.1) via point eigenvalues persists with a sharp resonance at $\rho = -1$ for (3.6), and the resulting bifurcation leads to 1d-targets and/or 1d-spirals depending on the symmetries of the associated eigenfunctions.

Next, we consider 1d-spirals. Symmetry enforces that Floquet multipliers $\rho \in \mathbb{R}^-$ of 1d-spirals on \mathbb{R} are double. This symmetry is also present for (3.6), and Remark 3.2 shows that a Floquet multiplier $\rho = -1$ therefore persists either as a double multiplier $\rho \in \mathbb{R}^-$ near -1 or will split into two complex conjugate multipliers. The same conclusion is true for the two multipliers near $\rho = -1$ that arise when the two boundary sinks undergo period doubling with simple multipliers at $\rho = -1$. We expect that the two multipliers near -1 will generically split, so that there is no sharp resonance at $\rho = -1$ for the truncated 1d-spiral of (3.6).

Lastly, we consider the absolute spectrum. The following corollary is a straightforward consequence of Theorem 3.

Corollary 3.3 (Generic absolute period doubling) *Resonant crossing of eigenvalues near the absolute spectrum at $\Lambda = \pm i\omega/2 + O(1/L)$ occurs in an open subset of 1-parameter families of reaction-diffusion systems.*

For 1d-spirals, we expect that, generically, the eigenvalues near the absolute spectrum will indeed move off the lines $\text{Im } \Lambda = \pm\omega/2$. For 1d-targets, we can, however, apply the same symmetry-based arguments as above which yield that the absolute eigenmodes decompose again into odd and even functions: This precludes movement of the associated Floquet multipliers off the lines $\text{Im } \Lambda = \pm\omega/2$, and we therefore obtain a sharp resonance with multipliers on these lines.

3.4 Nonlinear bifurcations of 1D sources, and the role of group velocity

We now analyse the period-doubling instability of 1d-targets and 1d-spirals on the unbounded real line $x \in \mathbb{R}$ that arises when essential spectrum crosses the imaginary axis. We are interested in constructing coherent structures which are periodic in time and spatially asymptotic to period-doubled wave trains in the far field as shown in Figure 2. Our goal is to derive bifurcation and bifurcation failure results which are valid uniformly in the size of the domain. Our approach will also allow us to gain insight into the role of transport as represented by the group velocity of the linear period-doubling modes.

Throughout this section, we assume the existence of a family of wave trains with nonzero group velocity c_g which undergo a period-doubling instability with dispersion curve $\Lambda_{\text{pd}}(\nu)$ which satisfies

$$\Lambda_{\text{pd}}(ik_*/2) = -i\omega_*/2, \quad c_g^{\text{pd}} = -\Lambda'_{\text{pd}}(ik_*/2) \neq 0, \quad \text{Re } \Lambda_{\text{pd}}(\nu) < 0 \text{ for all } \nu \neq ik_*/2.$$

Furthermore, we assume that the period-doubling bifurcation is supercritical (more precisely, that the period-doubling bifurcation in the space of spatially periodic functions is a supercritical pitchfork bifurcation). We will now state three theorems on period-doubling bifurcations from defects on \mathbb{R} which we shall prove later in this section.

Theorem 4 (Bifurcation from 1d-targets on \mathbb{R}) *Assume that there exists a 1d-target with $\Sigma_{\text{ext}} \cap i\mathbb{R} = \{0\}$ where $\Lambda = 0$ has multiplicity two, whose asymptotic wave trains undergo period doubling at $\mu = 0$. If $c_g^{\text{pd}} < 0$, then there exists a unique branch of bifurcating 1d-target patterns and a unique branch of 1d-spirals which are asymptotic to the period-doubled wave trains. If $c_g^{\text{pd}} > 0$, then 1d-target patterns and 1d-spirals that are asymptotic to the period-doubled wave trains do not exist near onset.*

Theorem 5 (Bifurcation from 1d-spirals on \mathbb{R}) *Assume that there exists a 1d-spiral with temporal frequency ω_* and with $\Sigma_{\text{ext}} \cap i\mathbb{R} = \{0\}$ where $\Lambda = 0$ has multiplicity two, whose asymptotic wave trains undergo period doubling at $\mu = 0$. If $c_g^{\text{pd}} < 0$, then there exists a unique branch, up to spatial reflection, of bifurcating solutions which are asymptotic to the period-doubled wave trains. The wave speed c_* of the bifurcating solutions is close to zero with $|c_*| \leq K|\mu|$ for some constant K , and their temporal frequency is close to $\omega_*/2$ in the comoving frame $\xi = x - c_*t$. If $c_g^{\text{pd}} > 0$, then standing or moving 1d-target patterns or 1d-spirals that are asymptotic to the period-doubled wave trains do not exist near onset.*

We have observed the bifurcation from 1d-spirals to moving period-doubled sources described in Theorem 5 in numerical simulations of the Rössler system; see the two rightmost plots in Figure 2.

While bifurcations from sources to period-doubled sources occur on \mathbb{R} if, and only if, the group velocity of the period doubling modes is directed towards the center of the defect, the following result shows that bifurcations from boundary sinks to period-doubled boundary sinks take place if, and only if, the group velocity is directed towards the boundary.

Theorem 6 (Bifurcation of boundary layers on \mathbb{R}^-) *Assume that there exists a 1d-boundary sink of (3.7) on \mathbb{R}^- such that $\Sigma_{\text{ext}} \cap i\mathbb{R} = \emptyset$. If $c_g^{\text{pd}} > 0$, then there exists a unique branch of bifurcating boundary sinks which are asymptotic to the period-doubled wave trains. If $c_g^{\text{pd}} < 0$, then boundary sinks that are asymptotic to the bifurcating period-doubled wave trains do not exist near onset.*

Combining the statements on the bifurcation of coherent structures and boundary sinks, we see that we cannot expect the simultaneous bifurcation to both coherent structures on \mathbb{R} and boundary layers on \mathbb{R}^- near the onset of an essential instability. In particular, if period-doubled sources bifurcate on \mathbb{R} , then period-doubled boundary sinks will not be present, and consequently the period-doubled sources will not persist on large bounded domains with Neumann boundary conditions. We refer to §5.4 for the analysis of a scenario where sources on \mathbb{R} persist on bounded domains due to instabilities of boundary sinks caused by point spectrum.

The results stated above reflect an intuitive heuristic picture of transport. The linear group velocity of eigenmodes encodes the direction towards which a localized perturbation constructed from the eigenmode will propagate. Thus, if we begin with a source on \mathbb{R} , then the group velocities c_g^{pd} of the period-doubling modes at $x = \pm\infty$ determine whether period-doubling modes can propagate towards the core of the source or not: If the group velocity c_g^{pd} at $x = \infty$ is positive, then the period-doubling modes cannot propagate towards the core, and a nonlinear bifurcation to a period-doubled pattern is not possible. The same arguments apply to boundary sinks provided we interpret the boundary as the core of the coherent structure. Since transport occurs either away from the boundary towards the core, or else away from the core towards the boundary, we cannot expect the simultaneous bifurcation of sources and boundary sinks.

In the remainder of this section, we sketch the proofs of Theorems 4-6. The arguments are similar to those given in [32], and we will therefore refer to [32] for the more technical aspects of the proofs. Since we are only interested in time-periodic solutions, we rewrite the reaction-diffusion equation as a first-order evolution equation in the spatial variable x ,

$$\begin{aligned} u_x &= v \\ v_x &= D^{-1}[\omega u_\tau - cv - f(u; \mu)], \end{aligned} \tag{3.8}$$

where $(u, v)(\cdot) \in H^1(S^1, \mathbb{R}^n) \times H^{1/2}(S^1, \mathbb{R}^n)$ are 2π -periodic in τ for each fixed x . We showed in [26, 32, 33] that coherent structures can be found as intersections of stable and unstable manifolds of the periodic orbits (in the evolution variable x) that correspond to the asymptotic wave trains. Essential instabilities of the wave trains correspond to pitchfork bifurcations of the corresponding periodic orbits. Although

(3.8) is ill-posed, the aforementioned stable and unstable manifolds exist, and the standard arguments for bifurcations in dynamical systems can be made rigorous [32, 33, 34, 35]. Equation (3.8) is invariant under the action of the symmetry group $\text{SO}(2)$ via the time shift action $\mathcal{S}_\theta : (u, v)(\tau) \mapsto (u, v)(\tau + \theta)$ for each fixed $\theta \in \text{SO}(2) \cong \mathbb{R}/2\pi\mathbb{Z}$. In particular, the subspace of solutions which are invariant under the shift $\mathcal{S}_\pi : \tau \mapsto \tau + \pi$ by half the period is invariant under the x -evolution. If we choose $\omega \approx \omega_*/2$, where ω_* is the temporal frequency of the primary source, then the primary wave trains and coherent structures lie in this fixed-point space, and we expect the period-doubled structures to bifurcate out of this subspace.

For the sake of clarity, we shall pretend in the rest of this section that the dynamics of (3.8) can be reduced to an appropriate six-dimensional invariant subspace, for instance by using a suitable combination of Fourier modes in the periodic variable τ . We assume that this subspace intersects the fixed-point subspace of the shift by half a period in a four-dimensional subspace. Since all solutions truly depend on τ , we may furthermore factor out the free action of $\text{SO}(2)/\mathbb{Z}_2$. We will now describe the dynamics of the reduced spatial dynamical system

$$U_x = F(U; \mu), \quad U \in \mathbb{R}^3 \times \mathbb{R}^2 \quad (3.9)$$

in the reduced phase space which we assume is given by $\mathbb{R}^3 \times \mathbb{R}^2$. As mentioned above, the technical tools necessary to extend the analysis of this "toy problem" to the full system (3.8) have been described in [32, 33, 34, 35] to which we refer for details.

The primary wave trains $u_{\text{wt}}(kx - \tau)$ correspond to relative periodic orbits of (3.8) with respect to the shift symmetry \mathcal{S}_θ and therefore, upon factoring out the shift, to equilibria of the reduced spatial system (3.9) in $\mathbb{R}^3 \times \{0\}$. Any neutral Floquet exponent $\Lambda \in i\omega\mathbb{Z}$ of the dispersion curve $\Lambda_*(i\gamma)$ of the linearization of the reaction-diffusion system (2.1) about the asymptotic wave train u_{wt} gives a neutral Floquet exponent $\nu = i\gamma \in i\mathbb{R}$ of the corresponding relative periodic orbit of (3.8). By assumption, there are precisely two such neutral eigenvalues, namely the phase eigenvalue $\Lambda = 0$ at $\nu = 0$ and the period-doubling mode $\Lambda = -i\omega_*/2$ at $\nu = ik_*/2$. Upon factoring out the shift symmetry $\text{SO}(2)/\mathbb{Z}_2$, we see that the eigenvalue $\Lambda = 0$, which corresponds to shifts, is removed, while the period-doubling eigenvalue gives a Floquet exponent at $\nu = 0$ with eigenvector contained in $\{0\} \times \mathbb{R}^2$. Inside the invariant subspace $\mathbb{R}^3 \times \{0\}$, the equilibrium is hyperbolic with one unstable eigenvalue if $c_g < 0$ and two unstable eigenvalues if $c_g > 0$; see [34]. Similarly, besides the neutral eigenvalue $\nu = 0$, the equilibrium has one unstable eigenvalue on $\{0\} \times \mathbb{R}^2$ if $c_g^{\text{pd}} > 0$ and one stable eigenvalue if $c_g^{\text{pd}} < 0$.

The reversers $\mathcal{R}_0 : (u, v) \mapsto (u, -v)$ and $\mathcal{R}_\pi := \mathcal{R}_0\mathcal{S}_\pi$ each fix a three-dimensional subspace in \mathbb{R}^6 which is invariant under the action of $\text{SO}(2)$, thus yielding a two-dimensional subspace in \mathbb{R}^5 whose intersection with the isotropy subspace $\text{Fix } \mathcal{S}_\pi$ is one-dimensional. Similarly, the space $\{(u, v); v = 0\}$ of functions that satisfy Neumann boundary conditions corresponds to a two-dimensional subspace in \mathbb{R}^5 which intersects $\text{Fix } \mathcal{S}_\pi$ in a line.

We now prove Theorem 4 for target patterns on \mathbb{R} . Before bifurcation for $\mu < 0$, 1d-targets are found as intersections in \mathbb{R}^5 of the two-dimensional space $\text{Fix } \mathcal{R}_0$ with the two-dimensional stable manifold of the equilibrium corresponding to the wave train with positive group velocity $c_g > 0$. The assumption that the extended point spectrum in the origin has multiplicity two means that the intersection of the tangent spaces of the stable manifold and $\text{Fix } \mathcal{R}_0$ is trivial and is broken with non-vanishing speed when we vary ω near $\omega_*/2$ [34].

First, assume $c_g^{\text{pd}} > 0$. From the preceding discussion of the dispersion relation, we see that the wave train is stable inside the one-dimensional center manifold for $\mu < 0$ before the onset of period doubling. The stable manifold of the asymptotic wave train can therefore be continued smoothly through the bifurcation as a center-stable manifold. The assumption of minimal extended point spectrum implies that the intersection between $\text{Fix } \mathcal{R}_0$ and the center-stable manifold of the equilibrium is transverse in the parameter ω at $\mu = 0$, and we conclude that the unique intersection persists through the bifurcation. Since this unique intersection is

given by the primary 1d-target pattern and therefore located inside $\text{Fix } \mathcal{S}_\pi$, we conclude that period-doubled target patterns cannot bifurcate.

Next, assume that $c_g^{\text{pd}} < 0$. The wave train is then unstable inside the center manifold for $\mu < 0$ before bifurcation, which means that the stable manifold continues continuously through the bifurcation as the strong stable fibre. At $\mu = 0$, the strong stable fibre of the primary wave train crosses $\text{Fix } \mathcal{R}_0$ transversely upon varying ω , and we conclude that the primary 1d-target persists. On the other hand, the strong stable fibre of the bifurcating period-doubled wave trains is $\sqrt{\mu}$ -close to the strong stable fibre of the primary wave train, and it therefore also crosses $\text{Fix } \mathcal{R}_0$ transversely for $\tilde{\omega} = \omega + O(\sqrt{\mu})$.

The same arguments apply when we replace $\text{Fix } \mathcal{R}_0$ by $\text{Fix } \mathcal{R}_\pi$, which completes the proof of Theorem 4.

The case of 1d-spirals is similar. The primary 1d-spirals are transverse intersection of the stable manifold of the wave train and the fixed-point space of the operator $\mathcal{R}_0 \mathcal{S}_{\pi/2}$, which acts as a reverser in $\text{Fix } \mathcal{S}_\pi$ but not in the entire phase space: Indeed, the flip symmetry of the shift $\mathcal{S}_{\pi/2}$ by half a period has order four after doubling the period and therefore cannot act as an involution when composed with the reverser $\mathcal{R}_0 : (u, v) \mapsto (u, -v)$. We therefore cannot expect to obtain period-doubled patterns as intersections with reversibility fixed-point spaces, instead the bifurcating patterns should drift. Thus, we transform into a comoving frame, include the wave speed $c \approx 0$ as an additional parameter, and seek intersections of the unstable manifold of the primary wave train with negative group velocity at $x = -\infty$ with the stable manifold of the primary wave train with positive group velocity at $x = \infty$. Since the intersection now occurs along flow lines of the differential equation, we lose one dimension for transversality, which is however compensated for by the additional parameter c . The existence and non-existence proofs for period-doubled sources proceeds now as before, and [29, Lemma 3.9] shows that the speed c of the bifurcating sources will be of the order $O(\mu)$. We omit the straightforward adaptation of the arguments.

It remains to discuss boundary sinks on \mathbb{R}_- , which we seek as transverse intersections of the unstable manifold of the wave trains at $x = -\infty$ with positive group velocity and the boundary subspace. Since $c_g > 0$ at $x = -\infty$, we have transversality of the intersection for fixed ω , and we consequently find a family of boundary sinks, parametrized by their temporal frequency ω . For $c_g^{\text{pd}} > 0$, we find a family of period-doubled boundary sinks by continuing the strong unstable manifold of the wave trains continuously through the bifurcation as the strong unstable manifold of the period-doubled wave trains after bifurcation. For $c_g^{\text{pd}} < 0$, period-doubled boundary sinks can bifurcate only near certain discrete values of ω where the transversality conditions are violated, and additional extended point spectrum occurs in the origin: An example where this can occur is near $k = 0$, and we refer to §5.4 for an analysis of the resulting scenario.

3.5 Nonlinear bifurcations of 1D sources on finite intervals

We now describe bifurcations on large bounded domains induced by the crossing of the absolute spectrum. Theorem 3 shows that there will be a large number of eigenvalues near each point of the absolute spectrum. Thus, for large domain diameters $L \gg 1$, we expect a sequence of bifurcations with a delayed onset $\mu_*(L) = \mu_*^\infty + O(1/L^2)$ of the instability compared with the crossing of the absolute spectrum at $\mu = \mu_*^\infty$. The small-amplitude regime of this bifurcation sequence can be analysed using the methods described in [36] for the analogous case of a pitchfork bifurcation (matching with the reversibility lines here is equivalent to matching with the boundary conditions described there). As in [36], we expect that the amplitude of the bifurcating pattern in the far field scales with $\sqrt{\mu - \mu_*(L)}L^{3/2}$. Instead of carrying out the analysis of the entire bifurcation sequence, we focus here on the first bifurcation.

We start with the case of a 1d-target pattern. If the absolute spectrum crosses the axis at $\rho = -1$, then §3.3 shows that clusters of Floquet multipliers pass through $\rho = -1$ on the real axis. From the expansion at the edge of the absolute spectrum [30, §5.4], we conclude that the first instability induced by the absolute

spectrum occurs on a two-dimensional center-eigenspace, with multipliers passing through -1 within $O(1/L)$ of each other as functions of the bifurcation parameter μ , where the reflection symmetry acts trivially in one direction and nontrivial in the other direction. In physical space, this can be interpreted as synchronizing the instability in the far field without phase shift or with a phase shift of π . The resulting bifurcation can be analysed using Lyapunov-Schmidt reduction (for finite large L) and exploiting the symmetry. We find again that 1d-target patterns bifurcate in the space of symmetric functions, while 1d-spirals, which are invariant under the flip symmetry $(x, t) \mapsto (-x, t + T)$, bifurcate in the space on which the symmetry acts nontrivially. We remark that the actual bifurcation is guaranteed on both spaces by degree arguments and the fact that the leading multipliers actually cross the imaginary axis. The absolute period-doubling of a 1d-target pattern already shows 'non-genericity' in the sense that we would typically expect the leading multipliers to be simple at resonance $\rho = -1$. The bifurcation analysis as described above remains valid only in a very small range of parameter values since the spectral gap to the next multiplier is only of order $1/L^2$.

Next, we consider 1d-spirals. For 1d-spirals, we cannot eliminate the translation symmetry by restricting to an appropriate fixed-point space since the isotropy of a 1d-spiral is trivial for each fixed time t , and instead need to consider the entire center manifold at once. Near a period-doubling bifurcation induced by the absolute spectrum, the linearization $\Phi'_T(u_*)$ has four Floquet multipliers in an $O(1/L^2)$ -neighborhood of the unit circle given by $\rho = 1$ from temporal translation, $\rho = O(e^{-\delta L})$ for the translation eigenvalue, and $\rho = -1 - \mu + O(1/L)$ for the period-doubling multiplier, which has geometric multiplicity two as shown in §3.3. The associated generalized eigenspace is therefore four-dimensional and can be parametrized by $\partial_t u_*$, $\partial_x u_*$ and the two period-doubling eigenfunctions v_{pd} and \bar{v}_{pd} . If we denote the associated coordinates by $(\tau, \xi, v) \in S^1 \times \mathbb{R} \times \mathbb{C}$ for the temporal phase τ , the spatial translation ξ , and the complex Hopf amplitude v , then we see upon using [40, Theorem 2.9] that the vector field on the center manifold for $L \gg 1$ is given by

$$\begin{aligned}\dot{\tau} &= \omega_L(\tau, \xi, v, \mu) \\ \dot{\xi} &= g_L(\tau, \xi, v, \mu) \\ \dot{v} &= h_L(\tau, \xi, v, \mu),\end{aligned}\tag{3.10}$$

where

$$\begin{aligned}\omega_L(\tau, \xi, 0, 0) &= \omega_* + O(e^{-\delta L}), & g_L(\tau, \xi, 0, 0) &= O(e^{-\delta L}), & g(\tau + 2\pi, \xi, v, \mu) &= g_L(\tau, \xi, v, \mu) \\ h_L(\tau, \xi, v, \mu) &= [i\omega_*/2 + O(\mu + e^{-\delta L})]v + \gamma_L(\tau, \mu)|v|^2v + O(|v|^5).\end{aligned}$$

We do not know whether the center manifold exists in a uniform neighborhood of the source or whether the Taylor expansion on the center manifold converges as $L \rightarrow \infty$. If we assume that the temporal average of $\gamma_L(\tau, 0)$ is strictly negative uniformly in $L \gg 1$, then we obtain $\dot{\xi} \approx \alpha_L \mu$ for a constant α_L due to resonant terms of the form $g_1 e^{i\tau} \bar{v}^2$ in $g_L(\tau, \xi, v, \mu)$ as in the analysis in the introduction or in [40, §7]. If α_L is not zero, the bifurcating 1d-spirals should therefore drift on $(-L, L)$ and eventually leave the local center manifold. We believe that this drift can be followed on a global group-invariant center manifold until the effects of the boundary become of the order of the drift speed μ .

4 Period doubling of spiral waves

The spectral analysis of planar spiral waves is in many respects analogous to that of 1d-spirals. We consider the reaction-diffusion equation (2.1)

$$u_t = D\Delta u + f(u; \mu), \quad (x, y) \in \mathbb{R}^2\tag{4.1}$$

first on the plane, and subsequently on large disks $B_R(0)$ of radius $R \gg 1$ together with appropriate boundary conditions. An Archimedean spiral wave is a rigidly rotating solution of the form

$$u(x, y, t) = u_*(r, \varphi - \omega t), \quad (x, y) = (r \cos \varphi, r \sin \varphi),$$

which converges to 1D wave trains u_{wt} ,

$$|u_*(r, \cdot - \omega_* t) - u_{\text{wt}}(k_* r + \theta(r) + \cdot - \omega_* t)|_{C^1(S^1)} \rightarrow 0 \text{ as } r \rightarrow \infty,$$

as $r \rightarrow \infty$, where $k_* \neq 0$ denotes the asymptotic wave number of the wave trains, and $\theta(r)$ is a smooth phase correction with $\theta'(r) \rightarrow 0$ as $r \rightarrow \infty$. We shall assume that the essential spectrum of the asymptotic one-dimensional wave train is simple at $\Lambda = 0$, and that the group velocity c_g of the wave train u_{wt} , computed in the laboratory frame, is positive.

Spiral waves are equilibria in the corotating frame $\psi = \varphi - \omega_* t$, where they satisfy the elliptic system

$$D \left[u_{rr} + \frac{1}{r} u_r + \frac{1}{r^2} u_{\psi\psi} \right] + \omega_* u_{\psi} + f(u(r, \psi); \mu) = 0 \quad (4.2)$$

with

$$|u_*(r, \cdot) - u_{\text{wt}}(k_* r + \theta(r) + \cdot)|_{C^1(S^1)} \rightarrow 0 \text{ as } r \rightarrow \infty. \quad (4.3)$$

The convergence assumed in (4.3) implies that the asymptotic shape of the spiral u_* is indeed given by the one-dimensional wave-train solution u_{wt} , while the asymptotic wave number k_* and the temporal frequency ω_* are related via $\omega_* = \omega_{\text{nl}}(k_*)$.

Next, we linearize (4.1) about the spiral wave in the corotating frame, which is equivalent to linearizing (4.2) about $u_*(r, \psi)$. The resulting operator \mathcal{L}_* is given by

$$\mathcal{L}_* u = D \left[u_{rr} + \frac{1}{r} u_r + \frac{1}{r^2} u_{\psi\psi} \right] + \omega_* u_{\psi} + f_u(u_*(r, \psi); \mu) u$$

which is a closed operator on $L^2(\mathbb{R}^2, \mathbb{R}^n)$. If we take the formal limit $r \rightarrow \infty$ in the eigenvalue equation

$$D \left[u_{rr} + \frac{1}{r} u_r + \frac{1}{r^2} u_{\psi\psi} \right] + \omega_* u_{\psi} + f_u(u_*(r, \psi); \mu) u = \Lambda u, \quad (4.4)$$

we obtain the limiting equation

$$D u_{rr} + \omega_* u_{\psi} + f_u(u_{\text{wt}}(k_* r + \psi); \mu) u = \Lambda u \quad (4.5)$$

with 2π -periodic boundary conditions in ψ . If we set $\psi \mapsto -\omega_* t$, we recover the Floquet eigenvalue problem (2.15) of the one-dimensional wave trains which we discussed in §2.2. The Floquet symmetry of the Floquet eigenvalue problem (2.15) is reflected in the invariance of the asymptotic spiral eigenvalue problem (4.5) under the substitution

$$u(r, \psi) \mapsto u(r, \psi) e^{i\ell\psi}, \quad \Lambda \mapsto \Lambda + i\omega_* \ell \quad (4.6)$$

for each $\ell \in \mathbb{Z}$. We emphasize that the transformation (4.6) for the essential spectrum will generate new curves of spectrum for (4.4): The new eigenvalues are generated by the asymptotic $\text{SO}(2)$ -symmetry of (4.4) and *not* by an artificial Floquet symmetry as for the wave trains: Indeed, the spiral wave is an equilibrium, and each Λ obtained from (4.6) belongs to a different eigenfunction.

We proved in [38] that these formal considerations can be made precise in the following sense. The operator $\mathcal{L}_* - \Lambda$ is Fredholm if, and only if, Λ does not belong to the Floquet spectrum of the linearized period map of the asymptotic wave trains in the laboratory frame, that is, if $e^{2\pi\Lambda/\omega_*}$ is not in the spectrum of the period map of

$$u_t = D u_{xx} + f_u(u_{\text{wt}}(k_* x - \omega_* t); \mu) u.$$

In particular, the essential spectrum is vertically periodic in the complex plane with period $i\omega_*$. Moreover, for spirals emitting wave trains, which by definition have $c_g > 0$ at $\nu = 0$, the essential spectrum of the

spiral wave in a neighborhood of the origin, and consequently all its vertical translates, moves into the left half-plane when \mathcal{L}_* is posed on the spaces with exponentially weighted norms

$$|u|_{L_\eta^2}^2 = \int_{\mathbb{R}^2} \left| u(x, y) e^{-\eta \sqrt{x^2 + y^2}} \right|^2 dx dy$$

for sufficiently small positive rates $\eta > 0$. We may therefore define the geometric and algebraic multiplicity of $\Lambda = 0$ and $\Lambda = \pm i\omega_*$ as eigenvalues of \mathcal{L}_* posed on L_η^2 for small $\eta > 0$: On this space, $\partial_\psi u_*$ provides an eigenfunction of \mathcal{L}_* with $\Lambda = 0$, while $\partial_x u_*$ and $\partial_y u_*$ generate eigenfunctions belonging to $\Lambda = \pm i\omega_*$. We proved in [38] that spiral waves are robust provided these eigenvalues are algebraically simple as eigenvalues in L_η^2 .

The preceding characterization of the essential spectrum of spiral waves by the spectrum of the asymptotic wave trains shows that essential spatio-temporal period-doubling of spiral waves is a robust phenomenon.

Corollary 4.1 (Robust period-doubling of planar spirals) *There exists an open class of one-parameter families of reaction-diffusion systems such that the essential spectrum of \mathcal{L}_* crosses the imaginary axis first at $\Lambda = \pm i\omega_*/2 + i\omega_*\ell$.*

In preparation for a discussion of the spectra of spirals under truncation to large bounded disks, we record that the absolute spectrum of (4.4) coincides with the absolute spectrum of the asymptotic wave trains, computed in the laboratory frame, which is again vertically periodic in the complex plane with period $i\omega_*$. In [38], we showed that for each $\Lambda \notin \Sigma_{\text{abs}}$ there exists an exponential weight η such that $\mathcal{L}_* - \Lambda$ is Fredholm with index zero on the space L_η^2 . We define the extended point spectrum as the set of $\Lambda \notin \Sigma_{\text{abs}}$ for which the kernel of $\mathcal{L}_* - \Lambda$ is nontrivial on L_η^2 , with η chosen as above. It is not difficult to see that the kernel does not depend on the choice of the weight [38].

The persistence of period doubling on large bounded disks of radius $R \gg 1$ with Neumann boundary conditions is now very similar in spirit to the situation in one space dimension. First, we address the persistence of the spiral wave on disks $B_R(0)$ for $R \gg 1$. Similarly to Theorem 1, we assume the existence of a 1D boundary sink that connects the asymptotic wave trains at $x = -\infty$ with Neumann conditions at $x = 0$ such that $\Lambda = 0$ does not belong to its extended point spectrum. Moreover, we assume robustness of the spiral on the plane, that is, we require that $\Lambda = 0$ is algebraically simple in L_η^2 for $\eta > 0$ small. Under these conditions, the spiral wave persists as a rigidly rotating solution of the reaction-diffusion system for all sufficiently large R [38].

Next, we consider the spectrum of the linearization (4.4) about the truncated spiral wave on $B_R(0)$ with Neumann conditions at $r = R$, for which a result completely analogous to Theorem 3 holds.

Theorem 7 ([38]) *Assume that the extended point spectrum of the spiral wave is discrete, then the spectrum of the truncated 2D spiral converges locally uniformly in the symmetric Hausdorff distance to the disjoint union of the absolute spectrum Σ_{abs} of the asymptotic wave trains, computed in the laboratory frame, and a discrete set of isolated eigenvalues with finite multiplicity. Convergence to the absolute spectrum is algebraic of order $O(1/R)$, and the number of eigenvalues inside any small disk that contains a point in the absolute spectrum converges to infinity as $R \rightarrow \infty$. The discrete part of the limiting spectrum is the union of the extended point spectrum of the spiral and the extended point spectrum of the boundary sink on \mathbb{R}^- . Convergence towards elements of the discrete part of the limiting spectrum is exponential in R , and the multiplicity of eigenvalues in a sufficiently small disk about an element of the extended point spectra converges to the sum of the multiplicities in the extended point spectra of planar spiral and boundary sink.*

Remark 4.2 *We remark that it has recently been shown numerically [41] and analytically [37] that infinitely many discrete eigenvalues in the extended point spectrum of spiral waves can accumulate at edges of the absolute spectrum.*

Corollary 4.3 (Absolute period-doubling on bounded domains) *Resonant crossing of eigenvalues at $\Lambda = \pm i\omega_*/2 + i\omega_*\ell + O(1/R)$ of spiral waves on disks of radius $R \gg 1$ occurs in an open subset of one-parameter families of reaction-diffusion systems.*

An interesting feature of period doubling of spiral waves is the shape of its period-doubling eigenfunctions. We first describe the shape of eigenfunctions for the essential spectrum (although this is somewhat irrelevant to bifurcations taking place on large disks). Consider the eigenvalue problem (2.8) of the wave train u_{wt} in the one-dimensional comoving frame and assume that it has period-doubling eigenvalues given by

$$\lambda(\nu) = -(c_{\text{g}}^{\text{pd}} - c_{\text{p}})(\nu - ik_*/2) + d(\nu - ik_*/2)^2 + O(|\nu - ik_*/2|^3), \quad c_{\text{p}} = \frac{\omega_*}{k_*}$$

for $\nu \approx ik_*/2$ with associated eigenfunctions given by

$$v(y) = e^{\nu y} u_{\text{pd}}(k_* y; \nu), \quad u_{\text{pd}}(k_* y; \nu) = u_{\text{pd}}(k_* y + 2\pi; \nu) \quad \forall y$$

when written in the variable $y = \xi/k_*$. In the laboratory frame $x = y + c_{\text{p}}t$, we obtain the critical dispersion curve

$$\Lambda(\nu) = -\frac{i\omega_*}{2} - c_{\text{g}}^{\text{pd}}(\nu - ik_*/2) + d(\nu - ik_*/2)^2 + O(|\nu - ik_*/2|^3) \quad (4.7)$$

with eigenfunctions

$$v(x, t) = e^{\Lambda(\nu)t} e^{\nu x} u_{\text{pd}}(k_*(x - c_{\text{p}}t); \nu).$$

The eigenfunction for the spiral is now obtained as in [31] by substituting $t = -\psi/\omega_*$ and $x = r$, which gives

$$u(r, \psi) = e^{-\Lambda(\nu)\psi/\omega_*} e^{\nu r} u_{\text{pd}}(k_* r + \psi; \nu)$$

for the solution of (4.4). We evaluate this expression at the critical wave number $\nu = ik_*/2$ to get

$$u_0(r, \psi) = e^{i(k_* r - \psi)/2} u_{\text{pd}}(k_* r + \psi) = e^{-i\psi/2} v_{\text{pd}}(k_* r + \psi) \quad (4.8)$$

where we substituted the real-valued function

$$v_{\text{pd}}(\xi) := e^{i\xi/2} u_{\text{pd}}(\xi)$$

with $v_{\text{pd}}(\xi + 2\pi) = -v_{\text{pd}}(\xi)$ for all ξ , which corresponds to the period-doubling solution of (2.5). Exploiting the Floquet symmetry (4.6), we find the additional eigenfunctions

$$u_{\ell}(r, \psi) = e^{i\psi(\ell-1/2)} v_{\text{pd}}(k_* r + \psi) \quad (4.9)$$

belonging to $\Lambda = -i\omega_*/2 + i\omega_*\ell$ for $\ell \in \mathbb{Z}$, and in particular the complex conjugate

$$u_1(r, \psi) = e^{i\psi/2} v_{\text{pd}}(k_* r + \psi) \quad (4.10)$$

of $u_0(r, \psi)$. To get real-valued solutions, we add up u_0 and u_1 and solve the time-dependent linearized problem with initial data $u_0 + u_1$ to get

$$u(r, \psi, t) = e^{-i\omega_* t/2} e^{-i\psi/2} v_{\text{pd}}(k_* r + \psi) + e^{i\omega_* t/2} e^{i\psi/2} v_{\text{pd}}(k_* r + \psi) = \cos\left(\frac{\psi + \omega_* t}{2}\right) v_{\text{pd}}(k_* r + \psi).$$

In the laboratory frame $\varphi = \psi + \omega_* t$, we finally obtain the real perturbation

$$u(r, \varphi, t) = \cos\left(\frac{\varphi}{2}\right) v_{\text{pd}}(k_* r + \varphi - \omega_* t). \quad (4.11)$$

If we formally add the solution (4.11) multiplied by a small amplitude $\sqrt{\epsilon}$ to the original spiral wave, we obtain

$$u_*(r, \varphi - \omega_* t) + \sqrt{\epsilon} \cos\left(\frac{\varphi}{2}\right) v_{\text{pd}}(k_* r + \varphi - \omega_* t) \quad (4.12)$$

in the spiral far field. In particular, the amplitude of the period-doubling mode vanishes along the stationary line $\varphi = \pi$, whilst the spiral is rotating. The temporal frequency of the perturbation is $\omega_*/2$ since v_{pd} has period 4π . The pattern described by (4.12) looks exactly like those observed experimentally in [24, 25, 43] and numerically in [13] and here in Figure 1.

Although this computation is formal, the shape of eigenfunctions resulting from the absolute spectrum on large bounded domains can be computed similarly: Assume therefore that $|c_g^{\text{pd}}| \ll 1$ as is the case, for instance, near spatially homogeneous oscillations. In this case, the absolute spectrum has a branch point Λ_{bp} close to the tip of the period-doubling instability at $\Lambda = i\omega_*/2 + \mu$. This branch point corresponds to a root of the equation $d\Lambda/d\nu = 0$, with $\Lambda(\nu)$ as in (4.7), and is therefore given by

$$\Lambda_{\text{bp}} = \frac{i\omega_*}{2} - \frac{[c_g^{\text{pd}}]^2}{4} + \mu, \quad \text{with} \quad \nu_{\text{bp}} = \frac{c_g^{\text{pd}}}{2d}.$$

Following the above computation gives

$$\cos(\varphi/2)e^{\nu_{\text{bp}}r}v_{\text{pd}}(k_*r + \varphi - \omega_*t)$$

for the perturbation of the primary spiral-wave profile. In particular, we observe the stationary line of vanishing amplitude for the period-doubling mode, and in addition an exponential decay or growth of the eigenfunction depending on whether the group velocity of the period-doubling mode is negative or positive, respectively.

At the onset of the absolute instability on large disks, there are five eigenvalues in the vicinity of the imaginary axis, namely $\Lambda = 0$ induced by rotation, $\Lambda = \pm i\omega_* + O(e^{-\delta L})$ induced by translation, and $\Lambda_{\text{pd}} = \pm i\omega_*/2 + O(1/L^2)$ near the branch point of the absolute spectrum that induces the period doubling of the wave trains. In [39], we showed that resonant Hopf bifurcations of this type will typically lead to a slow drift of the spiral wave with drift speed $O(\mu)$ (see also the discussion in the introduction §1). Based on this prediction, we verified that drift indeed occurs in the Rössler system and report on these computations in §6. Independently, drift was also observed numerically in [3].

We remark that the region of validity of our drift analysis is very small in parameter space since the eigenvalue at the edge of the absolute spectrum is $O(1/L^2)$ -close to other eigenvalues that subsequently cross the imaginary axis.

Lastly, we comment on the role played by the other eigenfunctions $u_\ell(r, \psi)$ given in (4.9). Proceeding as above, we see that the sum of the eigenfunctions $u_{\ell+1}$ and $u_{-\ell}$ for positive integers ℓ generates patterns of the form

$$u_*(r, \varphi - \omega_*t) + \sqrt{\epsilon} \cos\left(\frac{(2\ell+1)\varphi}{2}\right)v_{\text{pd}}(k_*r + \varphi - \omega_*t) \quad (4.13)$$

which exhibit $2\ell + 1$ stationary line defects at $\varphi = \frac{2n+1}{2\ell+1}\pi$ for $n = 0, \dots, 2\ell$. Interestingly, none of the associated eigenvalues at $\Lambda = i\omega_*(\ell + 1/2)$ affects the expected drift in any way as the resulting Hopf frequencies $\omega_H := \omega_*(\ell + 1/2)$ cannot satisfy the required resonance condition (1.3), except when $\ell = 0$ which is therefore solely responsible for the occurrence of drift.

5 Defects near period doubling of homogeneous oscillations

In this section, we study patterns that are created near the onset of period doubling of a family of wave trains. We restrict ourselves to the onset of period doubling at homogeneous oscillations where $k \approx 0$ and therefore $c_g = c_g^{\text{pd}} = 0$.

5.1 Derivation of amplitude equations

We shall assume that $u_0(\tau)$ has minimal period 2π and satisfies

$$\omega_0 u_\tau = f(u; \mu) \quad (5.1)$$

for $\mu = 0$ and some $\omega_0 \neq 0$. Furthermore, we assume that $\rho = 1$ and $\rho = -1$ are geometrically and algebraically simple Floquet multipliers of the linearization

$$\omega_0 u_\tau = f_u(u_0(\tau); 0)u$$

of (5.1) about $u_0(\tau)$; the associated nontrivial solutions of the linearization are given by $u'_0(\tau)$ and $u_{\text{pd}}(\tau)$, respectively. The associated solutions to the adjoint equation

$$\omega_0 w_\tau = -f_u(u_0(\tau); 0)^* w$$

will be denoted by $\psi_0(\tau)$ and $\psi_{\text{pd}}(\tau)$, respectively.

Simplicity of $\rho = 1$ implies that the periodic orbit $u_0(\tau)$ persists for all μ close to zero with temporal frequency $\omega = \omega_0(\mu)$, and we assume that the unique Floquet multiplier $\rho_{\text{pd}}(\mu)$ near $\rho = -1$ of the persisting wave train satisfies $\rho'_{\text{pd}}(0) < 0$. The simplicity of $\rho = 1$ also implies that the partial differential equation (PDE)

$$u_t = Du_{xx} + f(u; \mu) \quad (5.2)$$

with $\mu = 0$ has a one-parameter family of travelling waves $u(x, t) = u_0(\omega t - kx; k)$, defined for $|k| \ll 1$, near u_0 where $\omega = \omega_{\text{nl}}(k)$ with $\omega_{\text{nl}}(0) = \omega_0$ is a smooth, even function of k [34, §3.3]. We assume that the nonlinear dispersion relation $\omega_{\text{nl}}(k)$ is nondegenerate so that $\omega''_{\text{nl}}(0) \neq 0$. Lastly, the linearization

$$u_t = Du_{xx} + f_u(u_0(\omega_0 t); 0)u$$

of (5.2) about $u_0(\omega_0 t)$ can be reduced, via spatial Fourier transform, to the ODE

$$u_t = [D\nu^2 + f_u(u_0(\omega_0 t); 0)]u. \quad (5.3)$$

The simplicity of the multipliers $\rho = \pm 1$ implies that (5.3) has unique Floquet exponents, given by $\lambda_0 = d_0\nu^2 + O(\nu^4)$ and $\lambda_{\text{pd}} = \pi i + d_1\nu^2 + O(\nu^4)$ for appropriate constants $d_0, d_1 \in \mathbb{R}$, for $|\nu| \ll 1$, which correspond to $\rho = \pm 1$. We assume that $d_0, d_1 > 0$.

We are interested in coherent structures near the homogeneous oscillations. Thus, for ω close to ω_0 , we introduce the new time variable $\tau = \omega t$ and seek solutions $u(x, \tau)$ of the PDE

$$\omega u_\tau = Du_{xx} + f(u; \mu) \quad (5.4)$$

that are 4π -periodic in τ .

Theorem 8 *Under the above hypotheses, the following is true for all μ sufficiently close to zero and ω close to ω_0 : Solutions $u(x, \tau)$ of (5.4) with period 4π in τ whose time slices $u(x, \cdot)$ are, for each $x \in \mathbb{R}$, close to an appropriate τ -translate of $u_0(\cdot)$ are in one-to-one correspondence with small bounded solutions of the ODE*

$$\begin{aligned} \phi_x &= \kappa \\ \kappa_x &= \frac{1}{d_0} \left[-\bar{\omega} + \frac{1}{2}\omega''_{\text{nl}}(0)\kappa^2 + b_0 A^2 \right] + O(|A|^3 + |\kappa|^3 + B^2 + \bar{\omega}^2) \\ A_x &= B \\ B_x &= \frac{1}{d_1} [(-\rho'_{\text{pd}}(0)\mu + b_1\bar{\omega} + b_2\kappa^2 + b_3 A^2)A + b_4\kappa B] \\ &\quad + O(|A|(A^4 + A^2|\kappa| + \mu^2 + \bar{\omega}^2) + |B|\kappa^2 + B^2(|\kappa| + |A|)) \end{aligned} \quad (5.5)$$

where $\omega = \omega_0(\mu) + \bar{\omega}$. The right-hand side of (5.5) does not depend on ϕ and is equivariant under the reflection $(\phi, \kappa, A, B) \mapsto (\phi, \kappa, -A, -B)$, which corresponds to the time shift by 2π , and reversible under $x \mapsto -x$ with reverser $(\phi, \kappa, A, B) \mapsto (\phi, -\kappa, A, -B)$. The solution of (5.4) associated with a solution (ϕ, κ, A, B) of (5.5) has temporal period 2π if, and only if, $(A, B) = 0$.

Equation (5.5) is the steady-state equation associated with the formal amplitude equation¹

$$\begin{aligned}\phi_t &= d_0 \phi_{xx} - \frac{1}{2} \omega_{\text{nl}}''(0) \phi_x^2 + b_0 A^2 \\ A_t &= d_1 A_{xx} + \left[\rho'_{\text{pd}}(0) \mu - \hat{b}_1 \phi_{xx} + \hat{b}_2 \phi_x^2 + \hat{b}_3 A^2 \right] A + b_4 \phi_x A_x\end{aligned}\tag{5.6}$$

for the phase ϕ and the period-doubling mode A . A similar complex version of (5.6) has been analysed in [8, 9, 10] where it was derived from a combustion model using formal multi-scale expansions to describe the interaction of Burgers and Hopf modes. We also refer to [19] for the derivation of other amplitude equations for systems with conservation laws.

Before embarking on the proof of the preceding theorem, we consider spectral PDE stability of the bounded solutions $u_*(x, \tau)$ of (5.4) described by Theorem 8. A complex number λ is a Floquet exponent of $u_*(x, \tau)$ if, and only if, there exists a nontrivial 4π -periodic solution $u(x, \tau)$ of

$$\lambda u + \omega u_\tau = D u_{xx} + f_u(u_*(x, \tau); \mu) u.\tag{5.7}$$

Floquet exponents of $u_*(x, \tau)$ near the origin are captured by the following result.

Theorem 9 *Under the hypotheses of Theorem 8, assume that $U_*(x) = (\kappa_*, A_*, B_*)(x)$ is a small bounded solution of (5.5) corresponding to a 4π -periodic solution $u_*(x, \tau)$ of (5.4). If we write (5.5) as*

$$\begin{pmatrix} d_0 \phi_{xx} \\ d_1 A_{xx} \end{pmatrix} = G(\phi_x, A, A_x, \mu, \bar{\omega}),$$

then Floquet exponents λ of (5.7) near the origin are in one-to-one correspondence, counting multiplicity, with solutions λ near the origin of the reduced PDE eigenvalue problem

$$\begin{aligned}\begin{pmatrix} d_0 \phi_{xx} \\ d_1 A_{xx} \end{pmatrix} &= D_{(\kappa_*, A, B)} G(\kappa_*(x), A_*(x), B_*(x), \mu, \bar{\omega}) \begin{pmatrix} \phi_x \\ A \\ A_x \end{pmatrix} + \lambda \begin{pmatrix} 1 & 0 \\ b_1 A_*(x) & 1 \end{pmatrix} \begin{pmatrix} \phi \\ A \end{pmatrix} \\ &+ \lambda \left[\mathcal{O}(|\lambda| + |\mu| + |\bar{\omega}|) \begin{pmatrix} \phi \\ \phi_x \\ A \\ A_x \end{pmatrix} + \mathcal{O}(\|U_*\|) \begin{pmatrix} \phi_x \\ A \\ A_x \end{pmatrix} + \begin{pmatrix} \mathcal{O}(\|U_*\|) \\ \mathcal{O}(\|\kappa_*\|^2 + \|A_*\|^2 + \|B_*\|) \end{pmatrix} \Phi \right].\end{aligned}\tag{5.8}$$

Furthermore, $u_*(x, \tau)$ does not have any Floquet exponents in the right half-plane other than those captured by (5.8) (or those obtained from the trivial Floquet symmetry).

Proof of Theorems 8 and 9. We proceed using spatial dynamics as in [5, §8.1], and therefore write (5.4) as

$$\begin{aligned}u_x &= v \\ v_x &= D^{-1}[\omega u_\tau - f(u; \mu)]\end{aligned}\tag{5.9}$$

¹The coefficients \hat{b}_j can be obtained from the b_j 's upon solving the equation for κ in (5.5) for $\bar{\omega}$ and substituting into the equation for A .

on the space $\mathcal{X} := H_{\text{per}}^1(0, 4\pi) \times H_{\text{per}}^{1/2}(0, 4\pi)$. Thus, we regard (5.9) as a dynamical system in the spatial evolution variable x , acting on 4π -periodic functions $\mathbf{u} = (u, v) \in \mathcal{X}$ of the rescaled temporal variable τ . Important features of (5.9) are its equivariance under the shifts

$$\mathcal{S}_\phi : \mathcal{X} \longrightarrow \mathcal{X}, \quad \mathbf{u}(\cdot) \longmapsto \mathbf{u}(\cdot - \phi)$$

for each fixed $\phi \in [0, 4\pi]/\sim$ and reversibility in x with reverser $\mathcal{R} : (u, v) \mapsto (u, -v)$.

Equation (5.9) has, for $\mu = 0$ and $\omega = \omega_0$, an S^1 -group orbit of stationary solutions given by $\mathcal{S}_\phi \mathbf{u}_0$ where

$$\mathbf{u}_0 := \begin{pmatrix} u_0 \\ 0 \end{pmatrix}.$$

Each of these solutions has isotropy \mathbb{Z}_2 generated by $\mathcal{S}_{2\pi}$. We first concentrate on a neighborhood of \mathbf{u}_0 and write $\mathbf{u} = \mathbf{u}_0 + \mathbf{v}$ so that $\mathbf{v} \in \mathcal{X}$ satisfies

$$\mathbf{v}_x = \mathcal{B}_0 \mathbf{v} + (\omega - \omega_0) \mathcal{N}(\mathbf{u}_0 + \mathbf{v}) + \mathcal{G}(\mathbf{v}; \mu) \quad (5.10)$$

with

$$\begin{aligned} \mathcal{B}_0 &= \begin{pmatrix} 0 & 1 \\ D^{-1}[\omega_0 \partial_\tau - f_u(u_0(\cdot); 0)] & 0 \end{pmatrix}, & \mathcal{N} &= \begin{pmatrix} 0 & 0 \\ D^{-1} \partial_\tau & 0 \end{pmatrix} \\ \mathcal{G}(\mathbf{v}; \mu) &= \begin{pmatrix} 0 \\ -D^{-1}[f(u + u_0(\cdot); \mu) - f(u_0(\cdot); 0) - f_u(u_0(\cdot); 0)u] \end{pmatrix} \end{aligned}$$

for $\mathbf{v} = (u, v)$. This is the system considered in [5, §8.1]: Here, we have the additional simplification that both the wave number k_0 and the group velocity c_g vanish. As in [5, §8.1], the operator \mathcal{B}_0 is closed and densely defined on \mathcal{X} and has only discrete spectrum. Exploiting our hypotheses, we see that \mathcal{B}_0 has, in contrast to [5, §8.1], two geometrically simple eigenvalues at $\nu = 0$ with eigenfunctions $(u'_0, 0)$ and $(u_{\text{pd}}, 0)$ (compared with a unique geometrically simple eigenvalue in [5, §8.1]). Each of these eigenvalues has algebraic multiplicity two with generalized eigenfunctions given by $(0, u'_0)$ and $(0, u_{\text{pd}})$, respectively. The associated eigenfunctions of the adjoint operator \mathcal{B}_0^* are given by

$$\psi_0 = \begin{pmatrix} 0 \\ -D\psi_0 \end{pmatrix}, \quad \psi_1 = \begin{pmatrix} -D\psi_0 \\ 0 \end{pmatrix}, \quad \psi_0^{\text{pd}} = \begin{pmatrix} 0 \\ D\psi_{\text{pd}} \end{pmatrix}, \quad \psi_1^{\text{pd}} = \begin{pmatrix} D\psi_{\text{pd}} \\ 0 \end{pmatrix}, \quad (5.11)$$

where ψ_0 and ψ_{pd} have been defined at the beginning of §5.1. The remaining spectrum of \mathcal{B}_0 on \mathcal{X} is bounded away from the imaginary axis.

Using spatial center-manifold theory as in [5, §8.1], we conclude that there exists a four-dimensional center manifold associated with (5.9) which contains all solutions of (5.9) that stay near the S^1 -orbit $\{\mathcal{S}_\phi \mathbf{u}_0; \phi \in [0, 4\pi]/\sim\}$ of equilibria for all x . The center manifold can be constructed so that it is invariant under the shifts \mathcal{S}_θ and the reverser \mathcal{R} . In particular, the vector field on the center manifold is reversible and equivariant under shifts. Upon inspecting the operator \mathcal{B}_0 and exploiting the invariance under shifts in τ , we find that the center manifold can be parametrized by the coordinates (ϕ, κ, A, B) via

$$\mathbf{u} = \mathcal{S}_\phi \left[\begin{pmatrix} u_0(\mu) \\ 0 \end{pmatrix} - \kappa \begin{pmatrix} 0 \\ u'_0(\mu) \end{pmatrix} + A \begin{pmatrix} u_{\text{pd}}(\mu) \\ 0 \end{pmatrix} + B \begin{pmatrix} 0 \\ u_{\text{pd}}(\mu) \end{pmatrix} + \bar{\omega} \begin{pmatrix} u_\omega(\mu) \\ 0 \end{pmatrix} + \mathcal{H}_0(\kappa, A, B, \mu, \bar{\omega}) \right] \quad (5.12)$$

where $u_0(\mu)$ denotes the μ -dependent spatially homogeneous oscillation, $u_{\text{pd}}(\mu)$ is the μ -dependent eigenmode associated with $u_0(\mu)$ which causes period doubling at $\mu = 0$, and where we use the parameter $\bar{\omega} := \omega - \omega_0(\mu)$. The function u_ω is the unique 2π -periodic solution of the system

$$[\omega_0 \partial_\tau - f_u(u_0(\tau; \mu); \mu)] u_\omega = -u'_0 + \frac{\langle \psi_0, u'_0 \rangle_{L^2(0, 2\pi)}}{\langle \psi_0, Du'_0 \rangle_{L^2(0, 2\pi)}} Du'_0 \quad (5.13)$$

with $\langle u_\omega, u'_0 \rangle_{L^2(0,2\pi)} = 0$. The function \mathcal{H}_0 is smooth, takes values in the generalized hyperbolic eigenspace E^h of \mathcal{B}_0 , and its derivative with respect to each of its arguments vanishes at the origin $(\kappa, A, B, \mu, \bar{\omega}) = 0$. Indeed, in these coordinates, the shifts \mathcal{S}_θ are represented by

$$\mathcal{S}_\theta : (\phi, \kappa, A, B) \longmapsto (\phi + \theta, \kappa, A, B),$$

and equivariance implies that the reduced vector field, and the center-manifold parametrization \mathcal{H}_0 , can therefore not depend on ϕ , as claimed. The isotropy group generated by $\mathcal{S}_{2\pi}$ and the reverser \mathcal{R} are represented by

$$\mathcal{S}_{2\pi} : (\phi, \kappa, A, B) \longmapsto (\phi, \kappa, -A, -B), \quad \mathcal{R} : (\phi, \kappa, A, B) \longmapsto (\phi, -\kappa, A, -B).$$

In particular, the reduced vector field will be equivariant under $\mathcal{S}_{2\pi}$ and reversible under \mathcal{R} . We shall now argue that the vector field for (ϕ, κ, A, B) is necessarily of the form

$$\begin{aligned} \phi_x &= \kappa + g_1(\kappa, A, B, \mu, \bar{\omega}) \\ \kappa_x &= \frac{1}{d_0} \left[-\bar{\omega} + \frac{1}{2} \omega''_{\text{nl}}(0) \kappa^2 + b_0 A^2 \right] + \text{O}(|A|^3 + |\kappa|^3 + B^2 + \bar{\omega}^2) \\ A_x &= B + g_2(\kappa, A, B, \mu, \bar{\omega}) \\ B_x &= \frac{1}{d_1} \left[(-\rho'_{\text{pd}}(0) \mu + b_1 \bar{\omega} + b_2 \kappa^2 + b_3 A^2) A + b_4 \kappa B \right] \\ &\quad + \text{O}(|A|(A^4 + A^2 |\kappa| + \mu^2 + \bar{\omega}^2) + |B| \kappa^2 + B^2 (|\kappa| + |A|)) \end{aligned} \tag{5.14}$$

for appropriate constants $b_j \in \mathbb{R}$, where the functions g_1 and g_2 are smooth, respect the symmetries and the reverser, and their first two derivatives vanish at $(\kappa, A, B, \mu, \bar{\omega}) = 0$. Indeed, the linear terms in (5.14) can be computed as in [5, §8.1] by substituting (5.12) into (5.10) and projecting using the adjoint eigenfunctions (5.11). In particular, the coefficient b_1 is given by

$$b_1 = \frac{\langle \psi_{\text{pd}}, \partial_\tau u_{\text{pd}} - f_{uu}(u_0; 0) [u_\omega, u_{\text{pd}}] \rangle_{L^2(0,4\pi)}}{\langle \psi_{\text{pd}}, u_{\text{pd}} \rangle_{L^2(0,4\pi)}}. \tag{5.15}$$

The functions g_1 and g_2 must vanish to second order due to the facts that the diagonal of \mathcal{B}_0 vanishes and the nonlinearity appears only in the v -component. Checking compatibility of monomial terms with the involution $\mathcal{S}_{2\pi}$ and the reverser \mathcal{R} , we find that the equations for κ and B must be of the specified form. The special form of the equation for κ when $A = B = 0$ is a consequence of [5, §8.1] and our choice of $\bar{\omega}$ as the offset from the μ -dependent temporal frequency of spatially homogeneous oscillations. Lastly, to bring equation (5.14) into the form (5.5), we introduce the new coordinates

$$\tilde{\kappa} = \kappa + g_1(\kappa, A, B, \mu, \bar{\omega}), \quad \tilde{B} = B + g_2(\kappa, A, B, \mu, \bar{\omega}). \tag{5.16}$$

Upon dropping the tildes, we arrive at equation (5.5) as claimed, which completes the proof of Theorem 8.

To prove Theorem 9, we record that the solutions described by Theorem 8 are uniformly close to the homogeneous oscillations $u_0(\tau)$ whose Floquet multipliers are contained strictly inside the unit disk with the exception of multipliers close to $\rho = \pm 1$. Floquet multipliers near $\rho = \pm 1$ can be captured by a spatial center-manifold reduction for the eigenvalue problem

$$\mathbf{v}_x = [\mathcal{B}_0 + \bar{\omega} \mathcal{N} + \text{DG}(\mathbf{u}; \mu)] \mathbf{v} + \lambda \begin{pmatrix} 0 & 0 \\ D^{-1} \partial_\tau & 0 \end{pmatrix} \mathbf{v} \tag{5.17}$$

which is carried out simultaneously with the reduction for the existence problem (5.10). Following the same strategy as above, we find that the center manifold for the eigenvalue problem (5.17) about a solution \mathbf{u}

from (5.12) corresponding to a solution (κ_*, A_*, B_*) of (5.5) is parametrized by

$$\begin{aligned} \mathbf{v} = & \left[-\begin{pmatrix} u'_0 \\ 0 \end{pmatrix} - \kappa_* \begin{pmatrix} 0 \\ u''_0 \end{pmatrix} + A_* \begin{pmatrix} u'_{\text{pd}} \\ 0 \end{pmatrix} + B_* \begin{pmatrix} 0 \\ u'_{\text{pd}} \end{pmatrix} + \partial_\tau \mathcal{H}_0(\kappa_*, A_*, B_*, \mu, \bar{\omega}) \right] \Phi \\ & - \kappa \begin{pmatrix} 0 \\ u'_0 \end{pmatrix} + A \begin{pmatrix} u_{\text{pd}} \\ 0 \end{pmatrix} + B \begin{pmatrix} 0 \\ u_{\text{pd}} \end{pmatrix} + D_{(\kappa, A, B)} \mathcal{H}_0(\kappa_*, A_*, B_*, \mu, \bar{\omega}) \begin{pmatrix} \kappa \\ A \\ B \end{pmatrix} \\ & + \lambda \left[\begin{pmatrix} u_\omega(\mu) \\ 0 \end{pmatrix} \Phi + \mathcal{H}_{10} \begin{pmatrix} \kappa \\ A \\ B \end{pmatrix} + \mathcal{H}_{11}(\kappa_*, A_*, B_*, \mu, \bar{\omega}, \lambda) \begin{pmatrix} \Phi \\ \kappa \\ A \\ B \end{pmatrix} \right] \end{aligned} \quad (5.18)$$

where \mathcal{H}_{10} and \mathcal{H}_{11} map into the hyperbolic eigenspace E^h of \mathcal{B}_0 and where $H_{11}(0) = 0$. In particular, for $\lambda = 0$, we obtain precisely the linearization of the reduced vector field about (κ_*, A_*, B_*) , and it remains to calculate the λ -dependent terms. Using that \mathcal{H}_{10} maps into E^h and that $(u_\omega, 0) \in E^h$ by construction (5.13), we obtain the desired expression (5.8) upon substituting (5.18) into (5.7) and projecting using the adjoint eigenfunctions (5.11). We emphasize that the coefficient in front of the $\lambda A_* \Phi$ term is equal to b_1 as computed in (5.15). \blacksquare

The coefficients appearing in (5.5), and in particular the coefficient b_1 , are in general nonzero. It will often be more convenient to express the term $\bar{\omega}A$ in terms of $\kappa_x A$. Thus, we write (5.5) as

$$\begin{aligned} \phi_x &= \kappa \\ \kappa_x &= \frac{1}{d_0} \left[-\bar{\omega} + \frac{1}{2} \omega''_{\text{nl}}(0) \kappa^2 + b_0 A^2 \right] + \mathcal{O}(|A|^3 + |\kappa|^3 + B^2 + \bar{\omega}^2) \\ A_x &= B \\ B_x &= \left(-\frac{\rho'_{\text{pd}}(0)}{d_1} \mu + \tilde{b}_1 \kappa_x + \tilde{b}_2 \kappa^2 + \tilde{b}_3 A^2 \right) A + \tilde{b}_4 \kappa B \\ &\quad + \mathcal{O}(|A|(A^4 + A^2 |\kappa| + \mu^2 + \bar{\omega}^2) + |B| \kappa^2 + B^2 (|\kappa| + |A|)) \end{aligned} \quad (5.19)$$

where

$$\tilde{b}_1 := -\frac{d_0 b_1}{d_1}, \quad \tilde{b}_2 := \frac{b_2 + \frac{1}{2} \omega''_{\text{nl}}(0) b_1}{d_1}, \quad \tilde{b}_3 := \frac{b_3 + b_0 b_1}{d_1}, \quad \tilde{b}_4 := \frac{b_4}{d_1}.$$

The coefficients appearing in (5.19) have the following interpretation: b_0 describes how the temporal frequency of period-doubled spatially homogeneous oscillations changes with the amplitude of the period doubling mode. The coefficient \tilde{b}_2 encodes the wave number dependence of the onset of period doubling, and \tilde{b}_3 reflects whether the period doubling bifurcation is subcritical or supercritical. Lastly, \tilde{b}_4 gives the dependence of the linear group velocity of the period doubling mode on the wave number of the underlying wave train. We shall assume that the period doubling bifurcation is supercritical and that the homogeneous oscillations destabilize before the wave trains with nonzero wave number:

Hypothesis 1 *We assume that $\tilde{b}_2 > 0$ and $\tilde{b}_3 > 0$.*

Since we already assumed that $\omega''_{\text{nl}}(0) \neq 0$, we can arrange to have $\omega''_{\text{nl}}(0) > 0$, possibly after replacing κ by $-\kappa$. Using this normalization together with $\tilde{b}_3 > 0$, an appropriate change of the parameters and the dependent and independent variables transforms (5.19) into

$$\begin{aligned} \kappa_x &= -\bar{\omega} + \kappa^2 + bA^2 + \mathcal{O}(|A|^3 + |\kappa|^3 + B^2 + \bar{\omega}^2) \\ A_x &= B \\ B_x &= [-\mu + a\kappa_x + d\kappa^2 + A^2]A + c\kappa B + \mathcal{O}(|A|(A^4 + A^2 |\kappa| + \mu^2 + \bar{\omega}^2) + |B| \kappa^2 + B^2 (|\kappa| + |A|)) \end{aligned} \quad (5.20)$$

where we use the same letters for the new transformed variables and omitted the equation for ϕ as it decouples. Hypothesis 1 translates into $d > 0$.

The long wavelength scaling

$$(\kappa, A, B, \mu, \bar{\omega}, x) \longrightarrow \left(\epsilon\kappa, \epsilon A, \epsilon^2 B, \epsilon^2 \mu, \epsilon^2 \Omega, \frac{x}{\epsilon} \right) \quad (5.21)$$

transforms (5.20) into

$$\begin{aligned} \kappa_x &= -\Omega + \kappa^2 + bA^2 + O(\epsilon) \\ A_x &= B \\ B_x &= [-\mu + a\kappa_x + d\kappa^2 + A^2]A + c\kappa B + O(\epsilon). \end{aligned} \quad (5.22)$$

This system is equivariant under the reflection $\mathcal{S}_{2\pi} : (\kappa, A, B) \mapsto (\kappa, -A, -B)$ and reversible with reverser

$$\mathcal{R} : (\kappa, A, B) \longmapsto (-\kappa, A, -B).$$

We set $\epsilon = 0$ in the following and focus on the resulting system

$$\begin{aligned} \kappa_x &= -\Omega + \kappa^2 + bA^2 \\ A_x &= B \\ B_x &= [-\mu + a\kappa_x + d\kappa^2 + A^2]A + c\kappa B \end{aligned} \quad (5.23)$$

or alternatively, upon substituting the equation for κ_x into the last equation, on

$$\begin{aligned} \kappa_x &= -\Omega + \kappa^2 + bA^2 \\ A_x &= B \\ B_x &= [-(\mu + a\Omega) + (a + d)\kappa^2 + (1 + ab)A^2]A + c\kappa B. \end{aligned} \quad (5.24)$$

The reversibility of the full problem (5.22) will allow us to show persistence of the solutions of (5.23) that we shall construct below for $\epsilon > 0$.

Lastly, we discuss the PDE stability of bounded solutions $U_* = (\kappa_*, A_*, B_*)$ to (5.22) as given by Theorem 9. Using that any such solution U_* is of order ϵ as a solution to (5.20) due to the rescaling (5.21), it is not difficult to see that any eigenvalue λ of the reduced eigenvalue problem (5.8) which lies near the origin and has $\text{Re } \lambda \geq 0$ is necessarily of order $O(\epsilon^2)$; see [5, Proof of Lemma 8.2] for a similar argument. Thus, the rescaling (5.21) for U_* together with the rescaling

$$(\Phi, \kappa, A, B, \lambda, x) \longrightarrow \left(\Phi, \epsilon\kappa, \epsilon A, \epsilon^2 B, \epsilon^2 \Lambda, \frac{x}{\epsilon} \right) \quad (5.25)$$

for the linearization captures all unstable Floquet exponents near the origin, while transforming (5.8) into

$$\Lambda \begin{pmatrix} \frac{1}{d_0} & 0 \\ -aK_0 A_* & \frac{1}{d_1} \end{pmatrix} \begin{pmatrix} \Phi \\ A \end{pmatrix} = \left[\begin{pmatrix} \partial_{xx} - 2\kappa_* \partial_x & -2bA_* \\ (-2(a+d)\kappa_* A_* - cB_*) \partial_x & \partial_{xx} - c\kappa_* \partial_x + (\mu + a\Omega) - (a+d)\kappa_*^2 - (1+ab)A_*^2 \end{pmatrix} + O(\epsilon) \right] \begin{pmatrix} \phi \\ A \end{pmatrix} \quad (5.26)$$

for a certain constant $K_0 > 0$ that arises due to the coordinate transformations leading from (5.19) to (5.20). Since we will not need the precise value of K_0 , we will not compute it.

5.2 Wave trains

We first investigate equilibria of (5.23), which correspond to wave trains of the original reaction-diffusion system (5.4). Equilibria (κ, A, B) have $B = 0$ and satisfy

$$\Omega = \kappa^2 + bA^2, \quad [-\mu + d\kappa^2 + A^2]A = 0. \quad (5.27)$$

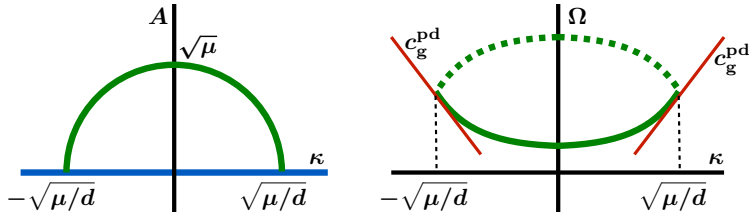


Figure 3: The bifurcation diagram of the wave trains [left] and their nonlinear dispersion relation [right] are shown: The solid dispersion curve is for $1 - bd > 0$, while the dashed curve is for $1 - bd < 0$.

Equilibria $U_0 = (\kappa, 0, 0)$ with $A = 0$ exist for all wave numbers κ with frequency offset given by $\Omega = \kappa^2$. Thus, their group velocity is given by

$$c_g^0 = \frac{d\Omega}{d\kappa} = 2\kappa.$$

The linearization of (5.23) about these solutions is given by

$$L_0 = \begin{pmatrix} 2\kappa & 0 & 0 \\ 0 & 0 & 1 \\ 0 & -\mu + d\kappa^2 & c\kappa \end{pmatrix}$$

from which we see that they are hyperbolic except when $\kappa = 0$ or $\kappa = \sqrt{\mu/d}$. The bifurcation at $\kappa = \sqrt{\mu/d}$ is a pitchfork which corresponds to the period doubling bifurcation which we analyse next.

The equilibria bifurcating at $\kappa = \sqrt{\mu/d}$ can be found by solving (5.27) with $A \neq 0$. We find equilibria

$$U_{\text{pd}} = \left(\kappa, \pm \sqrt{\mu - d\kappa^2}, 0 \right)$$

defined for $\kappa^2 < \mu/d$ where

$$\Omega = b\mu + (1 - bd)\kappa^2;$$

see Figure 3. The group velocity of the period doubled wave trains is therefore given by

$$c_g^{\text{pd}} = \frac{d\Omega}{d\kappa} = 2(1 - bd)\kappa.$$

Near $d\kappa^2 = \mu$, the linearization L_{pd} of (5.23) about U_{pd} has eigenvalues near 2κ and $c\kappa$ in addition to the pitchfork eigenvalue given by

$$\nu_{\text{pd}} = -\frac{c_g^{\text{pd}} A^2}{2c\kappa^2} + \mathcal{O}(A^3) = -\frac{(1 - bd)A^2}{c\kappa} + \mathcal{O}(A^3).$$

The spectrum of L_{pd} is illustrated in Figure 4. We remark that the spatial eigenvalue structure reveals in particular that the period doubled wave trains must be PDE unstable near onset for $c > 0$ and $1 - bd < 0$.

5.3 Coherent structures

Our goal in this section is to shed some light on the nature of the line defect that appears in Figure 1. The line defect mediates between a period-doubled wave train and its 2π -translate. Thus, we shall discuss coherent structures that are spatially asymptotic as $x \rightarrow \pm\infty$ to the period-two wave train U_{pd} and its 2π -translate $-U_{\text{pd}}$: These structures correspond to heteroclinic orbits between U_{pd} and $-U_{\text{pd}}$ of the spatial differential equation (5.24)

$$\begin{aligned} \kappa_x &= -\Omega + \kappa^2 + bA^2 \\ A_x &= B \\ B_x &= [-(\mu + a\Omega) + (a + d)\kappa^2 + (1 + ab)A^2]A + c\kappa B. \end{aligned} \tag{5.28}$$

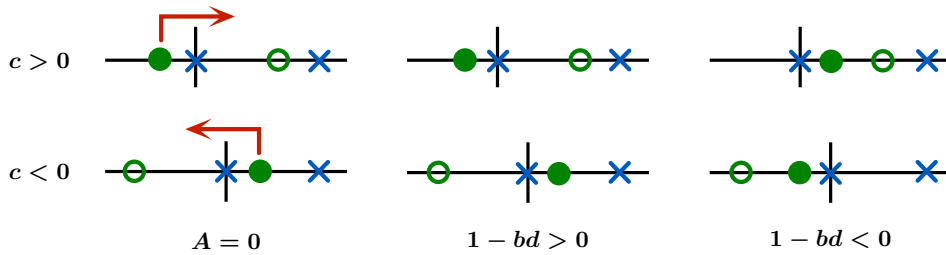


Figure 4: The spectra of the linearizations L_0 and L_{pd} of (5.23) about the equilibria U_0 [left] and U_{pd} [center and right], respectively, together with the phase eigenvalue at the origin from the trivial equation $\phi_x = \kappa$ are plotted for different signs of the parameters. The open and closed circles denote eigenvalues coming from the period doubling amplitude A , while crosses denote eigenvalues coming from the phase ϕ . The closed circle correspond to the eigenvalue ν_{pd} that triggers the period doubling bifurcation; the arrow denotes its movement upon decreasing κ through $\sqrt{\mu/d}$.

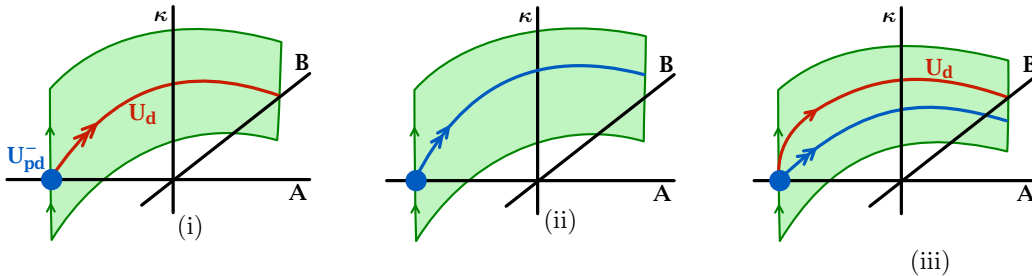


Figure 5: Figure (i) shows part of the reversible heteroclinic orbit U_d of (5.28) for $b = 0$ that connects the equilibrium U_{pd}^- to U_{pd}^+ . Figures (ii) and (iii) contain the unfolding for $b < 0$ and $b > 0$, respectively, upon setting $\Omega := b\mu$: The reversible heteroclinic orbit persists only for $b > 0$.

There are various limiting cases in which a perturbation analysis is possible. We focus on the perturbation from $b = 0$ as it is the most illuminating case.

When $b = 0$, (5.28) admits the semi-hyperbolic equilibria $U_{pd}^\pm = (0, \pm\sqrt{\mu}, 0)$ for $\Omega = 0$ and $\mu > 0$ which correspond to spatially-homogeneous period-doubled wave trains of the reaction-diffusion system (5.2). These equilibria are connected by the heteroclinic orbit

$$U_d(x) = \left(0, \sqrt{\mu} \tanh \sqrt{\frac{\mu}{2}} x, \frac{\mu}{\sqrt{2}} \operatorname{sech}^2 \sqrt{\frac{\mu}{2}} x \right);$$

see Figure 5(i). This orbit is reversible under the reverser $\mathcal{RS}_{2\pi} : (\kappa, A, B) \mapsto (-\kappa, -A, B)$. We discuss now in what sense the reversible connection U_d persists upon varying b near zero, while fixing all other parameters including μ . We focus on the persistence of reversible orbits which are obtained as intersections of unstable manifolds with the B -axis. The following analysis is similar to the one given in [34, §7].

The first case is $0 < b \ll 1$: We pick $\Omega = b\mu$ so that (5.28) becomes

$$\begin{aligned} \kappa_x &= \kappa^2 + b(A^2 - \mu) \\ A_x &= B \\ B_x &= [-\mu + (a+d)\kappa^2 + A^2 + ab(A^2 - \mu)]A + c\kappa B. \end{aligned} \tag{5.29}$$

In particular, the equilibrium $U_{pd}^- = (0, -\sqrt{\mu}, 0)$ persists as a semi-hyperbolic equilibrium for all $b > 0$. We wish to determine how the κ -component of the strong unstable manifold at $x = 0$ depends on b upon varying

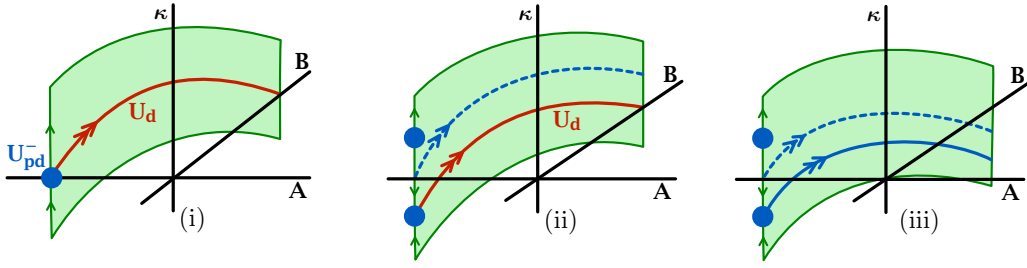


Figure 6: Figure (i) shows part of the reversible heteroclinic orbit U_d of (5.28) for $b = 0$ that connects the equilibrium U_{pd}^- to U_{pd}^+ . Figures (ii) and (iii) contain the unfolding for $b < 0$ and $b > 0$, respectively, upon setting $\Omega = b\mu + (1 - bd)\eta^2$ with $\eta \neq 0$: The reversible source persists for $b < 0$.

b near zero. To this end, we record that the adjoint variational equation

$$W_x = - \begin{pmatrix} 0 & 0 & 0 \\ 0 & 0 & 1 \\ cB_d(x) & [-\mu + 3A_d^2(x)]A & 0 \end{pmatrix}^* W$$

associated with the linearization of (5.29) about U_d at $b = 0$ has the solution $W(x) = (1, 0, 0)$. The Melnikov integral associated with the derivative of the right-hand side of (5.29) with respect to b is therefore given by

$$M := \int_{-\infty}^0 \left\langle W(x), (A_d^2(x) - \mu) \begin{pmatrix} 1 \\ 0 \\ a \end{pmatrix} \right\rangle dx = \int_{-\infty}^0 [A_d^2(x) - \mu] dx = -\sqrt{2\mu} < 0. \quad (5.30)$$

Thus, the unfolding of the heteroclinic orbit near $b = 0$ is as shown in Figure 5, and we conclude that the reversible heteroclinic orbit between the semi-hyperbolic equilibria U_{pd}^\pm persists only for $b > 0$, but not for $b < 0$. The resulting coherent structure of the reaction-diffusion system is a contact defect in the classification of [34] as it mediates between two wave trains with zero group velocity.

The remaining case is $-1 \ll b < 0$: We set $\Omega = b\mu + (1 - bd)\eta^2$ and treat η as independent parameter with $\eta \approx 0$ so that (5.28) becomes

$$\begin{aligned} \kappa_x &= -(1 - bd)\eta^2 + \kappa^2 + b(A^2 - \mu) \\ A_x &= B \\ B_x &= [-\mu - a(1 - bd)\eta^2 + (a + d)\kappa^2 + A^2 + ab(A^2 - \mu)]A + c\kappa B. \end{aligned} \quad (5.31)$$

The parameter η unfolds the saddle-node bifurcation occurring at $b = 0$, leading therefore to the equilibria

$$U_{pd}^\pm(\eta) = (\eta, \pm\sqrt{\mu - d\eta^2}, 0)$$

near U_{pd}^\pm . On account of the results in §5.2, we know that the equilibria $U_{pd}^\pm(\eta)$ have positive group velocity for $\eta > 0$ and negative group velocity for $\eta < 0$. We focus on finding reversible heteroclinic orbits that connect the hyperbolic equilibrium $U_{pd}^-(-\eta)$ at $x = -\infty$ to the hyperbolic equilibrium $U_{pd}^+(\eta)$ at $x = \infty$ for $\eta > 0$. The resulting coherent structure of the reaction-diffusion system is a source in the classification of [34] as it connects a wave train with negative group velocity at $x = -\infty$ to a wave train with positive group velocity at $x = \infty$. To find sources, we note that the behaviour of the κ -component of the strong unstable manifold under changes of b at $x = 0$ is, for $\eta = 0$, again determined by the Melnikov integral $M < 0$ in (5.30). Thus, as far as sources are concerned, the unfolding of the heteroclinic orbit near $b = 0$ is as shown in Figure 6: We conclude that, for each $b < 0$ close to zero, there is a unique $\eta > 0$ with a reversible heteroclinic orbit connecting $U_{pd}^-(-\eta)$ at $x = -\infty$ to $U_{pd}^+(\eta)$, while no such connection exists for $b > 0$.

Theorem 10 For $0 < b \ll 1$, the amplitude equation (5.28) has contact defects that connect the period-doubled spatially homogeneous wave train U_{pd} at $x = -\infty$ and its 2π -time translate at $x = \infty$. For $-1 \ll b < 0$, (5.28) admits sources that connect period-doubled wave trains $U_{\text{pd}}(x)$ with negative group velocity at $x = -\infty$ and to the reflected wave trains $U_{\text{pd}}(-x)$ with positive group velocity at $x = \infty$. For a, b, c and d sufficiently close to zero, both defects are spectrally stable.

Proof. The existence part has already been proved, and we therefore focus on spectral stability.

We consider sources first, and set $a = c = d = 0$, $b = -\delta$ and $\Omega = b + \eta^2 = -\delta + \eta^2$ for $\delta > 0$ small. We also rescale the A -equation so that $\mu = 1$. Thus, (5.31) becomes

$$\begin{aligned}\kappa_x &= -\eta^2 + \kappa^2 + \delta(1 - A^2) \\ A_x &= B \\ B_x &= [A^2 - 1]A\end{aligned}$$

so that $A_*(x) = \tanh(x/\sqrt{2})$ independently of η and δ . The source $U_d = (\kappa_*, A_*, \partial_x A_*)$ decays exponentially to zero as $x \rightarrow \pm\infty$ with rate independently of $\delta \geq 0$ since it lies by construction in the strong unstable and stable manifolds of the asymptotic semi-hyperbolic equilibria. The reduced PDE eigenvalue problem (5.26) about U_d is given by

$$\Lambda \begin{pmatrix} \phi \\ A \end{pmatrix} = \begin{pmatrix} d_0[\partial_{xx} - 2\kappa_*\partial_x] & 2\delta A_* \\ 0 & d_1[\partial_{xx} + 1 - A_*^2] \end{pmatrix} \begin{pmatrix} \phi \\ A \end{pmatrix}. \quad (5.32)$$

Since the constant functions are admissible eigenfunctions for sources according to the counting arguments presented in [34], we see that $\Lambda = 0$ is an eigenvalue with geometric multiplicity two. This is in line with [34, Lemma 4.4] which asserts that sources must have two eigenvalues at the origin. It remains to show that the algebraic multiplicity of $\Lambda = 0$ is two and that there are no other eigenvalues in the closed right half-plane. To prove this claim, we set $\delta = 0$ to get

$$\Lambda \begin{pmatrix} \phi \\ A \end{pmatrix} = \begin{pmatrix} d_0\partial_{xx} & 0 \\ 0 & d_1[\partial_{xx} + 1 - A_*^2] \end{pmatrix} \begin{pmatrix} \phi \\ A \end{pmatrix} =: \begin{pmatrix} \mathcal{L}_0 & 0 \\ 0 & \mathcal{L}_1 \end{pmatrix} \begin{pmatrix} \phi \\ A \end{pmatrix}. \quad (5.33)$$

Sturm–Liouville theory implies that \mathcal{L}_1 has a simple eigenvalue $\Lambda = 0$ and no other spectrum in the closed right half-plane. Similarly, \mathcal{L}_0 has the eigenvalue $\Lambda = 0$ with eigenfunction $\phi(x) = 1$ and no other spectrum in the closed right half-plane. Since the perturbation leading from (5.33) to (5.32) is small and decays with uniform exponential rate in x , we can apply standard Evans-function theory [15] to conclude that (5.32) with $0 < \delta \ll 1$ has precisely two eigenvalues near the origin, counting multiplicity, which are therefore given by the eigenvalues at $\Lambda = 0$ mentioned above. The same argument applies when perturbing from $(a, c, d) = 0$, which completes the proof for sources.

It remains to consider the contact defects. We set $a = c = d = 0$, $b = \delta$ and $\Omega = b = \delta$ for $\delta > 0$ small, and again rescale the A -equation so that $\mu = 1$. The existence problem (5.31) becomes

$$\begin{aligned}\kappa_x &= \kappa^2 - \delta(1 - A^2) \\ A_x &= B \\ B_x &= [A^2 - 1]A\end{aligned}$$

so that $A_*(x) = \tanh(x/\sqrt{2})$ independently of δ , and we get

$$\kappa_x = \kappa^2 - \delta \operatorname{sech}^2\left(\frac{x}{\sqrt{2}}\right).$$

We record for later use that the reversible contact-defect solution $\kappa_*(x)$ then satisfies

$$-\sqrt{2}\delta \leq \kappa_*(x) \leq 0, \quad x \geq 0$$

with $\kappa_*(0) = 0$ and $\kappa_*(x) = K_1/x^2 + O(1/x^3)$ as $x \rightarrow \infty$ for some $K_1 \leq 0$. The reduced PDE eigenvalue problem (5.26) about the contact defect is again given by

$$\Lambda \begin{pmatrix} \phi \\ A \end{pmatrix} = \begin{pmatrix} d_0[\partial_{xx} - 2\kappa_*\partial_x] & 2\delta A_* \\ 0 & d_1[\partial_{xx} + 1 - A_*^2] \end{pmatrix} \begin{pmatrix} \phi \\ A \end{pmatrix}. \quad (5.34)$$

As shown in [35, Theorem 3], contact defects have generically a single simple eigenvalue at the origin. Furthermore, it is a consequence of the results in [35] that the only admissible eigenfunctions of (5.34) are those that decay algebraically as $x \rightarrow \pm\infty$. We will therefore focus on the decoupled eigenvalue problem

$$\phi_{xx} - 2\kappa_*(x)\phi_x = \frac{\Lambda\phi}{d_0} \quad (5.35)$$

for ϕ and prove that it has no spectrum in the closed right half-plane for $\delta > 0$. Eigenfunctions belonging to nonzero eigenvalues Λ of (5.35) in the closed right half-plane decay necessarily exponentially with nonzero rate $\sqrt{\Lambda}$ and, using the algebraic convergence $\kappa_*(x) = K_1/x^2 + O(1/x^3)$ of the contact defect as $x \rightarrow \pm\infty$, we may therefore set

$$\Phi(x) := \exp\left(\int_{-\infty}^x \kappa_*(y) dy\right) \phi(x) \quad (5.36)$$

which transforms the eigenvalue problem for ϕ into the equivalent eigenvalue problem

$$\Phi_{xx} - \delta \operatorname{sech}^2\left(\frac{x}{\sqrt{2}}\right) \Phi = \frac{\Lambda\Phi}{d_0}$$

for Φ . For $\delta > 0$, there are no eigenvalues in the closed right half-plane, with the possible exception of the origin. We focus therefore on the eigenvalue problem (5.35) with $\Lambda = 0$, which is given by

$$\phi_{xx} - 2\kappa_*(x)\phi_x = 0. \quad (5.37)$$

For $\delta > 0$, the unique solution which decays algebraically as $x \rightarrow \infty$ is given by

$$\phi(x) = \int_{-\infty}^x \exp\left(\int_{-\infty}^y 2\kappa_*(z) dz\right) dy.$$

This solution is an eigenfunction provided it is odd as $\phi(x) = 1$ is the unique even solution of (5.37). Thus, we need $\phi_x(0) = 0$ but have

$$\phi_x(0) = \exp\left(\int_{-\infty}^0 2\kappa_*(z) dz\right) \neq 0$$

which proves that $\Lambda = 0$ is not an eigenvalue of (5.35). Lastly, the perturbation from $(a, c, d) = 0$ can be dealt with by regular perturbation theory using the Evans-function construction in [35]. ■

5.4 Boundary sinks

Lastly, we investigate the existence and stability of boundary sinks for Neumann boundary conditions. In other words, we seek solutions $U(x)$ of

$$\begin{aligned} \kappa_x &= -\Omega + \kappa^2 + bA^2 \\ A_x &= B \\ B_x &= [-(\mu + a\Omega) + (a + d)\kappa^2 + (1 + ab)A^2]A + c\kappa B \end{aligned} \quad (5.38)$$

for $x \leq 0$ so that $U(0)$ lies on the A -axis, corresponding to Neumann boundary conditions, and $U(x)$ converges to an equilibrium U_- of (5.38) with positive group velocity as $x \rightarrow -\infty$.

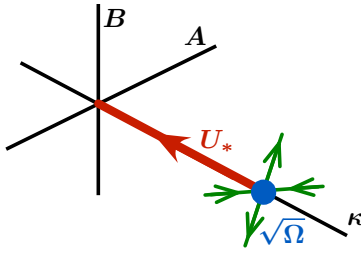


Figure 7: The boundary sink U_* which accommodates Neumann boundary conditions and the period-one wave train with nonzero wave number $\sqrt{\Omega}$ is shown for $\Omega > 1/d$.

We focus on the equilibria $U_0 = (\kappa, A, b) = (\sqrt{\Omega}, 0, 0)$ which correspond to the period-one wave trains with nonzero wave number $\sqrt{\Omega}$ and group velocity $c_g^0 = 2\kappa = 2\sqrt{\Omega} > 0$. In this case, the boundary sink is given explicitly by

$$U_*(x) = (\kappa, A, B)(x) = \left(-\sqrt{\Omega} \tanh(\sqrt{\Omega}x), 0, 0\right), \quad x \leq 0; \quad (5.39)$$

see Figure 7. The PDE stability of the boundary sink U_* can be analysed as follows. Evaluating (5.26) at $\epsilon = 0$, we find that the reduced eigenvalue problem associated with the boundary sink $U_* = (\kappa_*(x), 0, 0)$ is given by

$$\begin{aligned} \phi_{xx} - 2\kappa_*(x)\phi_x &= \frac{\Lambda}{d_0}\phi \\ A_{xx} - c\kappa_*(x)A_x + [\mu + a\Omega - (a+d)\kappa_*^2(x)]A &= \frac{\Lambda}{d_1}A \end{aligned}$$

on \mathbb{R}^- together with Neumann boundary conditions $\phi_x(0) = A_x(0) = 0$. The equation for ϕ decouples and coincides with the eigenvalue problem of Lax shocks of Burgers equation: in particular, there are no point eigenvalues in the closed right half-plane, and the essential spectrum consists of the curve $\Lambda/d_0 = -k^2 - 2\sqrt{\Omega}ik$ for $k \in \mathbb{R}$; see, for instance, [5, Lemma 8.2]. It remains to analyse the equation for A given by

$$\begin{aligned} A_{xx} + c\sqrt{\Omega} \tanh(\sqrt{\Omega}x)A_x + \left[\mu - d\Omega - (a+d)\Omega \operatorname{sech}^2(\sqrt{\Omega}x)\right]A &= \frac{\Lambda}{d_1}A, \quad x < 0 \\ A_x(0) &= 0. \end{aligned} \quad (5.40)$$

The essential spectrum of (5.40) is given by

$$\frac{\Lambda_{\text{ess}}(k)}{d_1} = \mu - \Omega d - k^2 - c\sqrt{\Omega}ik, \quad (5.41)$$

and we denote by

$$\frac{\Lambda_{\text{bp}}}{d_1} = \mu - \Omega \left(d + \frac{c^2}{4}\right) \quad (5.42)$$

the branch point of the linear dispersion relation Λ_{ess} . The point spectrum of (5.40) can also be calculated explicitly: Using the independent variable $z = \tanh(\sqrt{\Omega}x)$, real-valued solutions to (5.41) are given in terms of Ferrers functions which are appropriate linear combinations of the Associated Legendre functions [22, §5]. Using the results in [22, §5.12 and §5.15], we find that the point spectrum of (5.40) consists precisely of the points Λ_n given by

$$\frac{\Lambda_n}{d_1} = \mu - \Omega d + \frac{\Omega}{4} \left(\left[\sqrt{(c-1)^2 + 4(a+d)} - 1 - 4n \right]^2 - c^2 \right) \quad (5.43)$$

for those integers $n \geq 0$ for which

$$\sqrt{(c-1)^2 + 4(a+d)} \geq 1 + 4n. \quad (5.44)$$

In particular, the rightmost point eigenvalue Λ_0 is given by

$$\frac{\Lambda_0}{d_1} = \mu - \Omega d + \frac{\Omega}{4} \left(\left[\sqrt{(c-1)^2 + 4(a+d)} - 1 \right]^2 - c^2 \right), \quad (5.45)$$

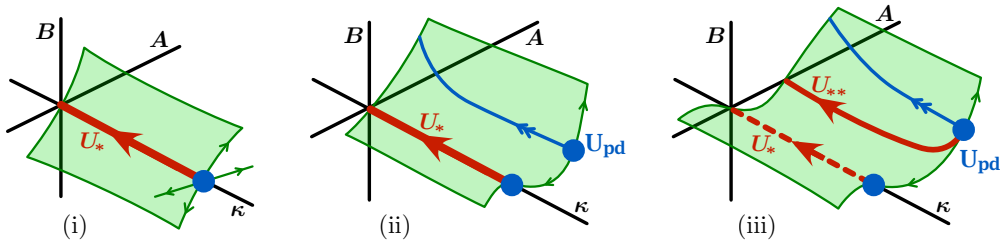


Figure 8: We illustrate case (2) ($c < 0$ and $\Lambda_{bp} < \Lambda_0 < \Lambda_{ess}$) for increasing μ under the assumption that the bifurcation associated with λ_0 is supercritical. The first instability occurs when $\Lambda_{ess} = 0$, leading in (ii) to a stable period-two wave train U_{pd} which does not persist under Neumann boundary conditions as there is no boundary sink available. When Λ_0 destabilizes, the stable boundary sink U_{**} bifurcates from U_* , and the period-two wave train U_{pd} persists now under Neumann boundary conditions due to the presence of U_{**} .

assuming that the term in the square brackets is positive.

We shall assume from now on that the group velocity c of the period doubling mode is negative so that $c < 0$. The period-one wave train U_- undergoes a pitchfork bifurcation at $\mu = \Omega d$ which, as outlined in §5.2, leads to the period-two wave train U_{pd} which has a nonzero A -component. We discuss now how this bifurcation, which occurs when the essential spectrum Λ_{ess} crosses the imaginary axis, interacts with the bifurcation of boundary sinks which occurs when the eigenvalue Λ_0 destabilizes. There are three relevant cases:

- (1) Λ_0 does not exist, that is, (5.44) is not met for $n = 0$;
- (2) $\Lambda_{bp} < \Lambda_0 < \Lambda_{ess}$;
- (3) $\Lambda_{ess} < \Lambda_0$.

Using $c \leq 0$, we see that the last case occurs for $a + d > 0$, while the eigenvalue Λ_0 disappears in the branch point Λ_{bp} when the term in the square brackets in (5.45) becomes zero. Since case (1) has already been discussed in §3.4, and case (2) is similar to (3), we concentrate in the following on (3) and refer to Figure 9 for an illustration of case (2).

Thus, assume that $c < 0$ and $\Lambda_{ess} < \Lambda_0$: Upon increasing μ , the boundary sink U_* destabilizes when $\Lambda_0 = 0$. In terms of the spatial ODE (5.38), this bifurcation manifests itself as a tangency of the unstable manifold of the equilibrium U_- as indicated in Figure 9(ii). We show in Lemma 5.1 below that this bifurcation can be supercritical, thus leading to a stable boundary sink U_{**} which connects U_- to the A -axis as illustrated in Figure 9(iii). Since the A -component of U_{**} is not zero, the boundary sink U_{**} will have period two, even though the period-two wave train U_{pd} has not yet bifurcated from U_- . A further increase of μ then leads to the period-two wave trains U_{pd} which persist under Neumann conditions thanks to the boundary sink U_{**} as indicated in Figure 9(iv). The characteristic feature of scenario (3) is therefore that the period doubling sets in first at the boundary, where it is also most pronounced during the entire bifurcation sequence. It remains to prove that the pitchfork bifurcation of the boundary sink is supercritical.

Lemma 5.1 *Assume that $b \leq 0$, $c < 0$, $a + d > 0$, and $1 + ab \geq 0$, then the pitchfork bifurcation of the boundary sink U_* which occurs when $\Lambda_0 = 0$ is supercritical.*

Proof. We need to prove that the part of the unstable manifold of U_- which lies in $A > 0$ has $B \geq 0$. Using the projective coordinate $w = B/A$, we arrive at the system

$$\begin{aligned} u_x &= -\Omega + u^2 + bA^2 \\ A_x &= Aw \\ w_x &= -(\mu + a\Omega) + (a + d)u^2 + (1 + ab)A^2 - cw - w^2. \end{aligned}$$

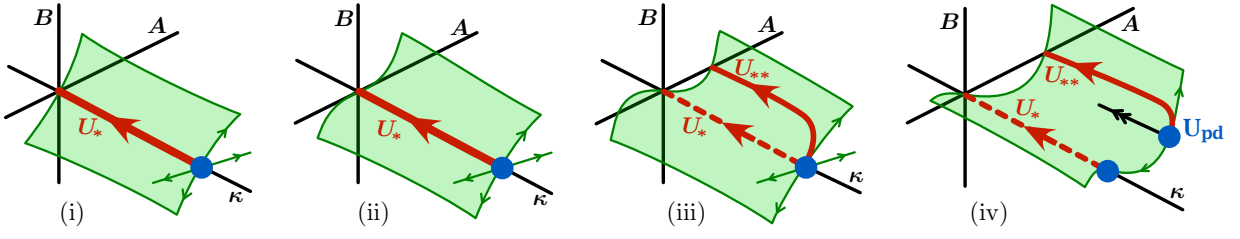


Figure 9: Case (3) ($c < 0$ and $\Lambda_{\text{ess}} < \Lambda_0$) is illustrated for increasing μ : The boundary sink U_* destabilizes in (ii) when the eigenvalue Λ_0 crosses the imaginary axis. This leads in (iii) to the existence of a stable period-doubled boundary sink U_{**} . The essential instability which occurs when $\Lambda_{\text{ess}} = 0$ leads then in (iv) to a stable period-two wave train U_{Pd} which persists under Neumann boundary conditions due to the presence of U_{**} .

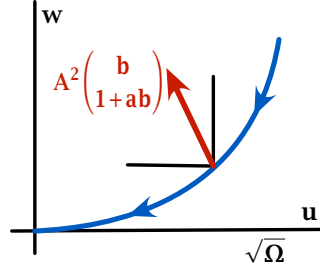


Figure 10: Proof of Lemma 5.1: If the tangent space angle $w(x)$ decreases monotonically, then the unstable manifold lies above the tangent space for $b < 0$ and $1 + ab > 0$.

If the solution that corresponds to the tangent space of the unstable manifold of U_- evaluated along the boundary sink U_* decreases monotonically for $x \in \mathbb{R}^-$, then the bifurcation will indeed be supercritical for $b < 0$ and $1 + ab > 0$ as outlined in Figure 10 since the nonlinear terms involving A point in the right direction. The tangent space of the unstable manifold of U_- evaluated along the boundary sink U_* satisfies the linearized equation

$$w_x = -(\mu + a\Omega) + (a + d)u_*^2(x) - cu_*(x)w - w^2.$$

We claim that $w_x < 0$ for all x for the solution that converges as $x \rightarrow -\infty$ to the tangent space of the unstable manifold of U_* . Firstly, for u near $\sqrt{\Omega}$, we write $u = \sqrt{\Omega} - h$ and $w(x) = w_* + W(x)$ where w_* is the unique positive solution of

$$-(\mu + a\Omega) + (a + d)\Omega - c\sqrt{\Omega}w_* - w_*^2 = 0 \quad (5.46)$$

which corresponds to the unstable eigenvector of the linearization of (5.38) about U_- . The resulting system for W is

$$W_x = (c\sqrt{\Omega} - 2w_*)W - \frac{h}{\sqrt{\Omega}}[2\Omega(a + d) + c\sqrt{\Omega}w_*] + O(h^2 + W^2).$$

Substituting (5.46), we get

$$W_x = (c\sqrt{\Omega} - 2w_*)W - \frac{h}{\sqrt{\Omega}}[\Omega(a + d) + \mu + a\Omega + w_*^2] + O(h^2 + W^2)$$

which means that $W_x < 0$ for $h > 0$ since the term in the square brackets turns out to be positive when $\Lambda_0 = 0$. A similar argument shows that the solution $w(x)$ satisfies $w_{xx}(x) < 0$ whenever $w_x(x) = 0$ which completes the proof. \blacksquare

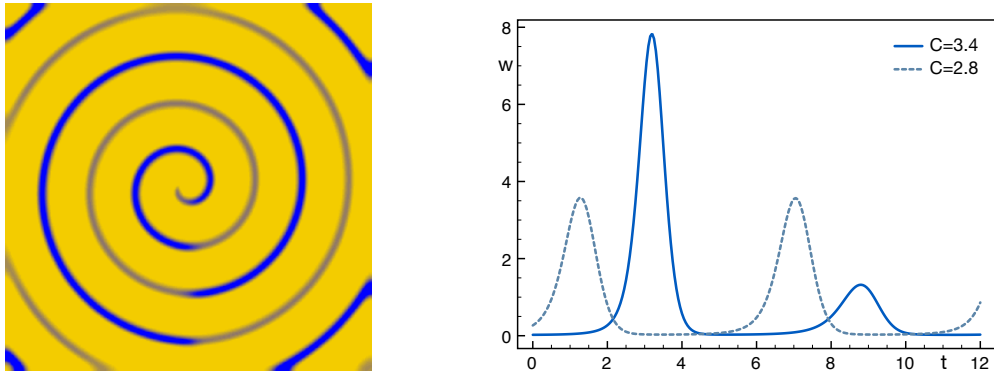


Figure 11: A contourplot of the w -component of the period-doubled spiral wave is plotted in the left figure for $C = 3.4$. To the right, the w -components of the spatially homogeneous oscillations are plotted as functions of time.

6 Period doubling of spirals in the Rössler system: A case study

In this section, we apply our findings to the planar 3-component partial differential equation

$$\begin{aligned} u_t &= 0.4 \Delta u - v - w \\ v_t &= 0.4 \Delta v + u + 0.2 v \\ w_t &= 0.4 \Delta w + uw - Cw + 0.2, \end{aligned} \quad (6.1)$$

written abstractly as

$$U_t = 0.4 \Delta U + f(U, C), \quad (6.2)$$

on a square $(x, y) \in (0, L)^2 \subset \mathbb{R}^2$ with Neumann boundary conditions. Kapral and coworkers [13] observed period-doubled spiral waves for (6.1) when changing the parameter C in the interval $(2.8, 3.4)$; see Figures 1 and 11.

Spatially homogeneous solutions of (6.1) satisfy the Rössler equation

$$\begin{aligned} u_t &= -v - w \\ v_t &= u + 0.2 v \\ w_t &= uw - Cw + 0.2 \end{aligned} \quad (6.3)$$

which is known to exhibit periodic solutions which undergo a period-doubling sequence beginning at $C = 2.83$; see Figure 11. The periodic solutions of (6.3) are accompanied by 1D wave trains $U(kx - \omega t)$ of (6.2) with nonzero wave number k which can be found as 2π -periodic solutions of the travelling-wave ODE

$$0.4 k^2 U_{xx} + \omega U_x + f(U, C) = 0, \quad x \in \mathbb{R}. \quad (6.4)$$

In the remainder of this section, we report on numerical computations for (6.1) and (6.4). We used Barkley's finite-difference code EZSPIRAL [2] for direct numerical simulations of spiral-wave solutions to (6.1), typically with $L = 250$, and the boundary-value solver AUTO97 [4] for all computations relating to the travelling-wave ODE (6.4). In particular, the absolute and essential spectra of wave trains are computed with AUTO97 using the algorithms outlined in [27, 31].

The nonlinear dispersion relation $\omega = \omega_{\text{nl}}(k)$ of the wave trains of (6.4) is shown in Figure 12. Note that their phase velocity $c_p = \omega/k$ and their group velocity $c_g = d\omega/dk$ have opposite sign: Since the 2D spiral waves select the wave trains with positive group velocity, the wave trains in the far field of the 2D spirals travel towards the core rather than towards the boundary.

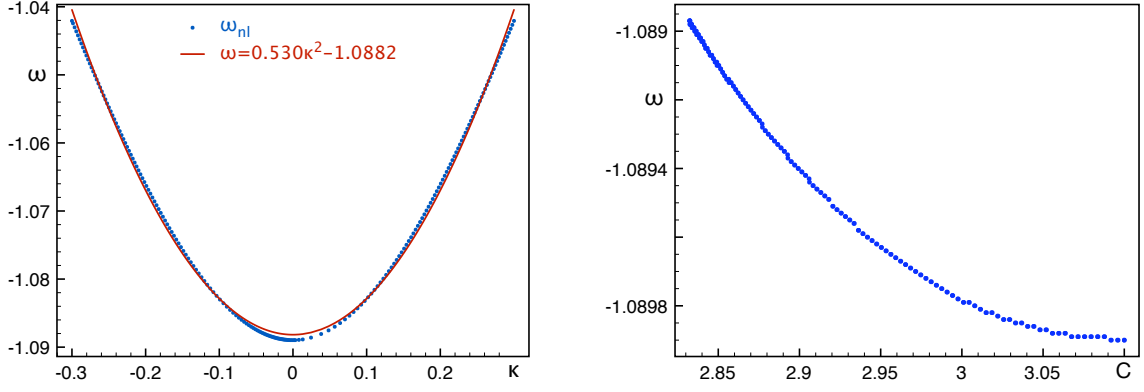


Figure 12: In the left figure, we plot the nonlinear dispersion relation $\omega_{nl}(k)$ of the 1D wave trains of (6.4) for $C = 2.8324$, i.e. at the period-doubling bifurcation. To the right, the temporal frequency ω of the period-doubled spatially homogeneous oscillations is plotted against the parameter C . Since onset occurs at $C = 2.834$, the bifurcation is supercritical, whence $\hat{b}_3 > 0$ in (6.5). Since the frequency decreases with the period-doubling amplitude, we see that the coefficient b_0 in (6.5) is negative.

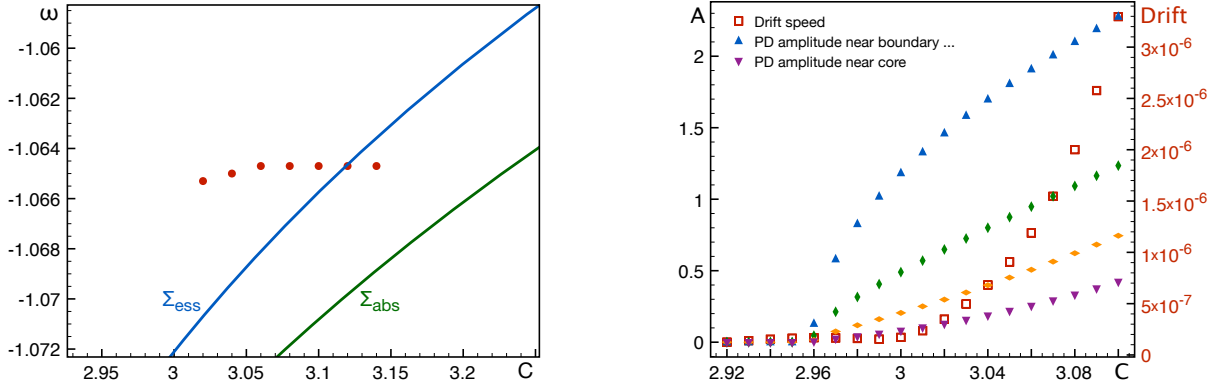


Figure 13: The left plot shows the onset of absolute and essential period-doubling instabilities of 1D wave trains with temporal frequency ω as a function of C , and it also contains the frequencies selected by the 2D spiral waves of (6.1). The right figure shows the drift velocity of the spiral tip (right y-axis) and the period-doubling amplitude A of the spirals (left y-axis) evaluated at different points along a ray from the core to the boundary as functions of the parameter C [see text for details].

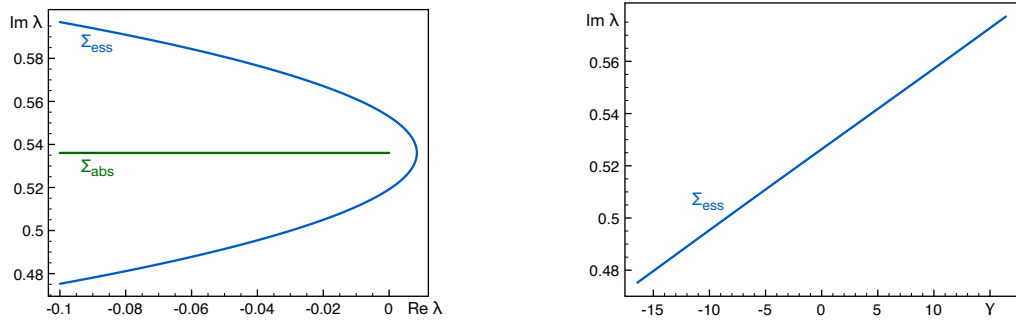


Figure 14: Absolute and essential period-doubling spectra of the spiral waves are shown [left]. The right plot shows the linear period-doubling dispersion relation with $\text{Im } \lambda_{pd}$ plotted against the associated wave number k : The linear group velocity c_g^{pd} is therefore negative.

Next, we plot in Figure 13 the curves where the essential and absolute spectra of the 1D wave trains with frequency ω cross the imaginary axis: These instabilities are caused by period-doubling modes with negative linear group velocity $c_g^{\text{pd}} < 0$; see Figure 14. Direct numerical simulations of (6.1) allow us to determine the temporal frequencies selected by spiral waves for different values of C , which are also shown in Figure 13. The associated spatial wave number of the wave trains in the far field is $k \approx 0.2$ which is close to zero in line with the observation that the period doubling bifurcations are organized by spatially homogeneous oscillations.

The closeness to spatially homogeneous oscillations allows us to investigate the nature of the line defect that is visible in Figure 11 by applying the results of §5.3 about coherent structures: Figure 12 shows that the coefficient b arising in (5.28) is negative, and Theorem 10 then implies that the line defect in Figure 11 is a source, rather than a contact defect. The analysis in §5.3 predicts a $\tanh(x)$ profile of the period-doubling mode across the line defect which has indeed been measured in [13, (2) and Figure 3] based on numerical simulations of (6.1). We refer to [44] for an analysis of line defects based on interpreting spirals as a field of coupled oscillators.

To determine when and how the spiral waves destabilize upon increasing C , we fix points (x_0, y_0) in the domain and record the time series $w_*(x_0, y_0, t)$ of the spiral wave. We then compute the difference between consecutive maxima of the time series which we use as a measure for the period-doubling amplitude. This computation is done for five points (x_j, y_j) which are spaced equi-distantly on a ray that connects the spiral core to the boundary and avoids the line defect. Since our theoretical results predict that period-doubled spirals ought to drift, we also computed the spiral tip and its drift velocity. The results are shown in Figure 13: The indications are therefore that period doubling of spirals sets in at $C \approx 2.96$. The instability appears to set be most visible at the boundary, with a square-root type behaviour reminiscent of pitchfork and Hopf bifurcations, and less pronounced towards the core. The spiral does begin to drift, but the drift velocity is very small and there is no clear onset visible.

We now discuss the different possible mechanisms outlined in §4 that may be responsible for the observed period doubling in the Rössler system. Firstly, we plot in Figure 14 representative absolute and essential spectra of the asymptotic 1D wave trains. Lemma 2.3 asserts that the absolute spectrum arising due to period-doubling bifurcations of wave trains near spatially homogeneous oscillations has to lie on the symmetry line $\text{Im } \lambda = \omega/2$, and this is indeed what happens here for the spatial wave numbers $k \approx 0.2$ selected by the spirals. Figure 14 also shows that the linear group velocity c_g^{pd} of the period doubling modes is negative. However, both absolute and essential spectra are still in the left half-plane when the period doubling sets in at $C = 2.96$. Furthermore, due to $c_g^{\text{pd}} < 0$, the absolute eigenmodes decay towards the boundary which appears to contradict Figure 13 which seems to imply that period doubling is more pronounced at the boundary. Thus, the bifurcation does not seem to be caused directly by the absolute spectrum.

The second possibility is that the instability is caused by point eigenvalues that emanate from the branch point located at the edge of the absolute spectrum due to curvature effects of the Laplacian; see Remark 4.2. We have evaluated numerically the criterion derived in [37, §IV] using the algorithm described there and found that, in the notation of [37], $\Phi = \pi$ which means that no point eigenvalues arise near the branch point.

This leaves the last option, namely that period doubling is caused by point eigenvalues of the boundary sink. We have discussed this case in §5.4 for boundary sinks in the near-spatially homogeneous case and shown that these sinks can indeed possess isolated point eigenvalues that are in resonance with $i\omega/2$. In particular, the scenario described in Figure 9 is consistent with the numerical observations reported in Figure 13, and therefore provides the likeliest explanation for the occurrence of period doubling in the Rössler system: As seen from Figure 9(iii), the period-doubling amplitude is most visible at the boundary, whilst decreasing towards the core. Since the adjoint eigenfunction associated with the translational eigenmodes of the spiral wave decreases exponentially towards the boundary, we expect that the drift coefficient is exponentially small

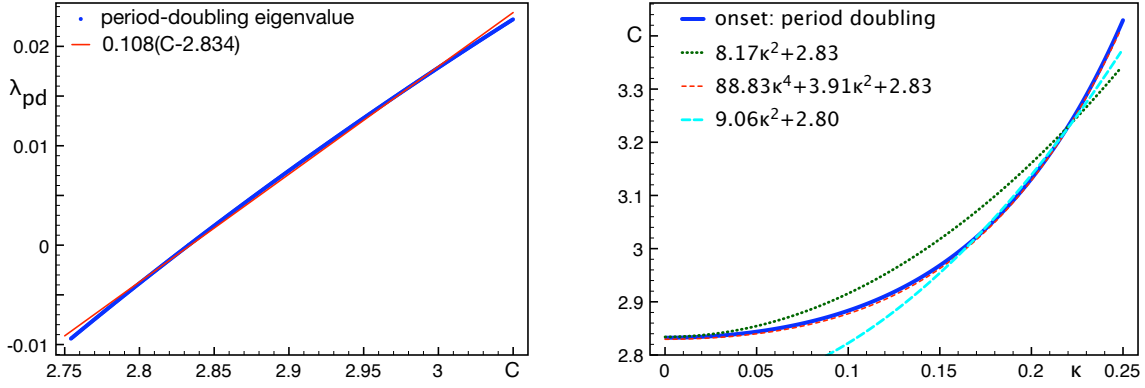


Figure 15: In the left figure, we plot the period-doubling Floquet exponent λ_{pd} of the spatially homogeneous wave trains of (6.3) as a function of the parameter C . The right figure shows the period-doubling bifurcation curve of wave trains to (6.4) with wave number k together with various curve fits.

in the domain diameter which may explain the slow drift observed in Figure 13.

To further corroborate this conclusion, we exploit that the wave trains selected by the spiral waves have wave numbers near zero and are therefore close to spatially homogeneous oscillations. Thus, if we can determine the coefficients appearing in the reduced eigenvalue problem (5.40) of the boundary sinks, then we can calculate the approximate location of the rightmost eigenvalue Λ_0 given in (5.45) and the expected onset of period doubling. The unscaled version (5.5) of the amplitude equations is given by

$$\begin{aligned} d_0\kappa_x &= -\bar{\omega} + \frac{1}{2}\omega''_{nl}(0)\kappa^2 + b_0A^2 \\ d_1A_{xx} &= [-\mu + \hat{b}_1\kappa_x + \hat{b}_2\kappa^2 + \hat{b}_3A^2]A + b_4\kappa A_x. \end{aligned} \quad (6.5)$$

We remark that the coefficients b_0 and \hat{b}_3 do not enter into the calculations presented in §5.4 but Figure 12 indicates that \hat{b}_3 is positive as required. The coefficient b_0 is relevant for the line defect of the period doubled spiral and has already been discussed above. The parameter μ will be replaced later by an appropriate expression in C .

Firstly, we note that $d_0 = d_1 = 0.4$ are equal to the diffusion coefficient in (6.1) since the diffusion matrix is a multiple of the identity. The fit to the nonlinear dispersion relation presented in Figure 11 gives $\frac{1}{2}\omega''_{nl}(0) = 0.530$. The coefficient \hat{b}_1 can be computed numerically by evaluating (5.15): Since the diffusion matrix in (6.1) is a multiple of the identity, it follows from (5.13) that $u_\omega = 0$. After calculating the adjoint solution ψ_{pd} of the linearization of (6.3) about the homogeneous oscillation, we obtain $\hat{b}_1 = 0.925$. The coefficient b_4 is equal to the slope of the linear group velocity of the period doubling mode, considered as a function of the wave number k of the underlying wave train: our computation of this slope gives $b_4 = -0.74$; see [27] for the relevant algorithms. Next, we need to express the bifurcation parameter μ in (6.5) by an appropriate expression in C : To this end, we calculated in Figure 15 the period-doubling Floquet exponent of the homogeneous oscillations as a function of C . A least-square fit gives $\lambda_{pd} = 0.108(C - 2.834)$, and therefore $\mu = 0.108(C - 2.834)$ since μ in (6.5) and λ_{pd} in the reduced eigenvalue problem appear with the same coefficient. Summarizing the results obtained so far, we arrive at the equation

$$\begin{aligned} 0.4\kappa_x &= -\bar{\omega} + 0.530\kappa^2 \\ 0.4A_{xx} &= [-0.108(C - 2.834) + 0.925\kappa_x + \hat{b}_2\kappa^2]A - 0.74\kappa A_x. \end{aligned} \quad (6.6)$$

It remains to determine the coefficient \hat{b}_2 which measures the dependence of the onset of period doubling on the wave number k of the underlying wave train of (6.4). This relation, together with various curve fits, is plotted in Figure 15. We recall that the spirals select wave numbers of around $k = 0.203$: In this region,



Figure 16: A snap shot of a period-doubled spiral wave with five interacting line defects is plotted for the Rössler system (6.1) with $C = 3.4$.

however, there is unfortunately no accurate fit of the required form $C - 0.2834 = \hat{b}_2 k^2$. Thus, we do not seem to be in the region where the approximation by (6.5) is valid. We therefore proceed as follows: Firstly, we may take $\hat{b}_4 = 9.06$ which corresponds to a quadratic fit in the interval $k \in (0.15, 0.25)$. Alternatively, we replace the $\hat{b}_2 \kappa^2$ term in (6.6) by $88.8\kappa^4 + 3.91\kappa^2 + 2.83$ which is an excellent fit of Figure 15. In the latter case, our formula (5.45) for the rightmost boundary-sink eigenvalue is no longer valid, and we determine this eigenvalue numerically using finite differences. Both approximations result in an eigenvalue Λ_0 that destabilizes prior to the essential spectrum: The predicted parameter values for the onset of the point instability are $C = 2.99$, when taking $\hat{b}_4 = 9.06$, and $C = 3.06$ for the approximation by the quartic polynomial, compared with the value $C = 2.96$ indicated by the direct simulations from Figure 13. Thus, while the predicted and measured values for onset disagree, the amplitude equation does predict that the instability is caused by a point eigenvalue of the boundary sink rather than by the absolute spectrum.

7 Discussion

In summary, we investigated period-doubling bifurcations of 1D sources and 2D spiral waves. The proposed explanation for spatio-temporal period doubling of spiral waves appears to be consistent with numerical simulations of the Rössler system. We also found numerical evidence that period-doubled spirals drift, as predicted, and we clarified the nature of the line defects that appear in the period-doubled pattern by showing that these can be sources or reversible contact defects.

Still, large parts of our analysis are only formal. For instance, the prediction of drift for truncated sources is based on the reduced equation (3.10) on an appropriate center manifold: It is not clear whether the center-manifold reduction is valid in a uniform region near the source, and not even whether the Taylor jet of the reduced vector field has a limit as the domain diameter goes to infinity. Similarly, we are currently not able to analyse the nonlinear bifurcation of spiral waves on the plane or on large bounded disks.

The remaining open problems we would like to mention pertain to the line defects. As indicated by (4.13) and shown in Figure 16, it is possible to excite several line defects near onset. Neighbouring line defects typically attract each other which eventually leads to pairwise annihilation. We expect that the time scales of this interaction depend strongly on whether they involve sources or contact defects. Another open problem is the transverse instability of line defects observed in [25].

Acknowledgments. B. Sandstede was partially supported by a Royal Society–Wolfson Research Merit Award and by the NSF through grant DMS-0203854. A. Scheel was partially supported by the NSF through grant DMS-0203301.

A Spectra of sources on large bounded domains

We outline the proof of Theorem 3. Suppose that $u_*(x, t)$ is a source on $(-L, L)$ obtained from Theorem 1 as the concatenation of a source on \mathbb{R} and two boundary sinks. The linearization of (3.6) about u_* is given by

$$\begin{aligned} v_t &= Dv_{xx} + f_u(u_*(x, t); \mu)v, & x \in (-L, L) \\ 0 &= v_x(\pm L, t), \end{aligned}$$

and we denote its evolution by Φ'_t . Floquet multipliers ρ can be found by seeking nontrivial solutions v_0 to $\Phi'_T v_0 = \rho v_0$, where $T = 2\pi/\omega_*$ denotes the temporal period of the source u_* . Writing

$$v(x, t) = e^{\Lambda t} u(x, t)$$

for $v(x, t) = \Phi'_t v_0$, we see that $\rho = e^{\Lambda T}$ is a Floquet multiplier if, and only if, $u(x, t)$ satisfies

$$\begin{aligned} u_t &= Du_{xx} + f_u(u_*(x, t); \mu)u - \Lambda u, & x \in (-L, L) \\ 0 &= u_x(\pm L, t), \end{aligned} \tag{A.1}$$

with $u(x, t)$ being T -periodic in t . As in [34, §4.1], we write (A.1) as

$$\begin{pmatrix} u_x \\ v_x \end{pmatrix} = \begin{pmatrix} 0 & 1 \\ D^{-1}[\partial_t - f_u(u_*(x, t); \mu) + \Lambda] & 0 \end{pmatrix} \begin{pmatrix} u \\ v \end{pmatrix}, \tag{A.2}$$

with $\mathbf{u} = (u, v) \in \mathcal{X} := H_{\text{per}}^{1/2}(0, T) \times L^2_{\text{per}}(0, T)$ for all x , together with the boundary conditions $\mathbf{u}(\pm L) \in H_{\text{per}}^{1/2}(0, T) \times \{0\}$.

We want to prove that the Floquet spectrum of the truncated source u_* is the union of two disjoint sets: One of these approaches the absolute spectrum of the asymptotic wave trains $u_{\text{wt}}(k_*x - \omega_*t)$ in the symmetric Hausdorff distance as $L \rightarrow \infty$, whilst the other one converges to the union of the extended point spectra of the source on \mathbb{R} and the two boundary sinks. This issue has previously been addressed in [30] in the case where the linearized problem (A.2) is an ODE.

The convergence proof for the absolute spectrum in [30, §5.3] involves only exponential dichotomies and Lyapunov–Schmidt reduction, and therefore carries over immediately to (A.2) once the absolute spectrum of the wave trains u_{wt} is identified: For constant-coefficient problems

$$\mathbf{u}_x = \mathcal{A}(\Lambda)\mathbf{u}, \quad \mathbf{u} \in \mathbb{R}^{2n},$$

the absolute spectrum is given by

$$\Sigma_{\text{abs}} = \{\Lambda \in \mathbb{C}; \operatorname{Re} \nu_n = \operatorname{Re} \nu_{n+1}\},$$

where $\nu_j = \nu_j(\Lambda)$ with $j = 1, \dots, 2n$ are the eigenvalues of the matrix $\mathcal{A}(\Lambda)$, ordered with increasing real part. The corresponding definition for (A.2) uses spatial Floquet exponents instead of eigenvalues: We consider the asymptotic $2\pi/k_*$ -periodic system

$$\mathbf{u}_x = \begin{pmatrix} 0 & 1 \\ D^{-1}[\partial_t - f_u(u_{\text{wt}}(k_*x - \omega_*t); \mu) + \Lambda] & 0 \end{pmatrix} \mathbf{u}$$

whose spatial Floquet exponents ν are found by seeking solutions $\mathbf{u} \in \mathcal{X}$ of the form

$$\mathbf{u}(x, t) = e^{\nu x} \mathbf{u}_0(k_*x - \omega_*t)$$

where \mathbf{u}_0 is 2π -periodic in its argument. As shown in [33, Proposition 2.10 and §4] or [34, §3.4], there are infinitely many spatial Floquet exponents $\nu_j(\Lambda)$ for each fixed Λ which, alternatively, can also be found as roots ν of the function $\mathcal{D}(\Lambda, \nu)$. Ordering the resulting roots ν_j by increasing real part, we end up with the absolute spectrum (2.23) of the wave trains in the laboratory frame. With this identification, the proofs given in [30, §5.3] for the absolute spectrum carry over to (A.2).

It remains to prove that the remaining spectrum converges to the union of the extended point spectra of the source on \mathbb{R} and the boundary sinks. There are two different proofs that give this result: Firstly, we may invoke [28] where the spectrum of concatenated multi-pulses was investigated, using again only exponential dichotomies and Lyapunov–Schmidt reduction. An alternative proof uses the same topological winding-number arguments based on Evans functions as in [30, §4.3] but now applied to a finite-dimensional Galerkin approximation of (A.2): It is a consequence of the results proved in [18, 33] that a sufficiently high-dimensional Galerkin approximation captures all eigenvalues of the truncated source.

References

- [1] D. Barkley. Euclidean symmetry and the dynamics of rotating spiral waves. *Phys. Rev. Lett.* **72** (1994) 164–167.
- [2] D. Barkley. *EZSPIRAL: A code for simulating spiral waves*. University of Warwick, 2002.
- [3] J. Davidsen, R. Erichsen, R. Kapral and H. Chaté. From ballistic to Brownian vortex motion in complex oscillatory media. *Phys. Rev. Lett.* **93** (2004) 018305.
- [4] E. Doedel, A.R. Champneys, T.F. Fairgrieve, Y.A. Kuznetsov, B. Sandstede and X. Wang. *AUTO97: Continuation and bifurcation software for ordinary differential equations (with HOMCONT)*. Technical report, Concordia University, 1997.
- [5] A. Doelman, B. Sandstede, A. Scheel and G. Schneider. The dynamics of modulated wave trains. *Memoirs Amer. Math. Soc.* (accepted).
- [6] B. Fiedler, B. Sandstede, A. Scheel and C. Wulff. Bifurcations from relative equilibria of noncompact group actions: skew products, meanders, and drifts. *Doc. Math.* **1** (1996) 479–505.
- [7] R.A. Gardner. On the structure of the spectra of periodic travelling waves. *J. Math. Pures Appl.* **72** (1993) 415–439.
- [8] E.A. Glasman, A.A. Golovin and A.A. Nepomnyashchy. Instabilities of wavy patterns governed by coupled Burgers equations. *SIAM J. Appl. Math.* **65** (2004) 230–251.
- [9] A.A. Golovin, B.J. Matkowsky, A. Bayliss and A.A. Nepomnyashchy. Coupled KS–CGL and coupled Burgers–CGL equations for flames governed by a sequential reaction. *Physica D* **129** (1999) 253–298.
- [10] A.A. Golovin, A.A. Nepomnyashchy and B.J. Matkowsky. Traveling and spiral waves for sequential flames with translation symmetry: Coupled CGL–Burgers equations. *Physica D* **160** (2001) 1–28.
- [11] M. Golubitsky, V. LeBlanc and I. Melbourne. Meandering of the spiral tip—an alternative approach. *J. Nonlinear Sci.* **7** (1997) 557–586.
- [12] M. Golubitsky, I. Stewart and D.G. Schaeffer. *Singularities and groups in bifurcation theory II*. Springer, New York, 1988.
- [13] A. Goryachev, H. Chaté and R. Kapral. Synchronization defects and broken symmetry in spiral waves. *Phys. Rev. Lett.* **80** (1998) 873–876.
- [14] W. Jahnke, W.E. Skaggs and A.T. Winfree. Chemical vortex dynamics in the Belousov-Zhabotinsky reaction and in the two-variable Oregonator mode. *J. Chem. Phys.* **93** (1989) 740–749.

- [15] T. Kapitula and B. Sandstede. Stability of bright solitary-wave solutions to perturbed nonlinear Schrödinger equations. *Physica D* **124** (1998) 58–103.
- [16] H. Kielhöfer. *Bifurcation theory: An introduction with applications to PDEs*. Springer, New York, 2004.
- [17] G. Li, Q. Ouyang, V. Petrov and H.L. Swinney. Transition from simple rotating chemical spirals to meandering and travelling spirals. *Phys. Rev. Lett.* **77** (1996) 2105–2108.
- [18] G.J. Lord, D. Peterhof, B. Sandstede and A. Scheel. Numerical computation of solitary waves in infinite cylindrical domains. *SIAM J. Numer. Anal.* **37** (2000) 1420–1454.
- [19] P.C. Matthews and S.M. Cox. Pattern formation with a conservation law. *Nonlinearity* **13** (2000) 1293–1320.
- [20] A. Mielke. A spatial center manifold approach to steady bifurcations from spatially periodic patterns. In: "Dynamics in Dissipative Systems: Reductions, Bifurcations and Stability" (Eds.: G. Dangelmayr, B. Fiedler, K. Kirchgässner and A. Mielke). Pitman Research Notes **352** (1996) 209–262.
- [21] S. Nettesheim, A. von Oertzen, H.H. Rotermund and G. Ertl. Reaction diffusion patterns in the catalytic CO-oxidation on Pt(110)-front propagation and spiral waves. *J. Chem. Phys.* **98** (1993) 9977–9985.
- [22] F.W.J. Olver. *Asymptotics and special functions*. Academic Press, New York, 1974.
- [23] Q. Ouyang and J.M. Flesselles. Transition from spirals to defect turbulence driven by a convective instability. *Nature* **379** (1996) 143–146.
- [24] J.-S. Park and K.J. Lee. Formation of spiraling line-defect and its meandering transition in a period-2 medium. *Phys. Rev. Lett.* **88** (2002) 224501.
- [25] J.-S. Park, S.-J. Woo and K.J. Lee. Transverse instability of line defects of period-2 spiral waves. *Phys. Rev. Lett.* **93** (2004) 098302.
- [26] D. Peterhof, B. Sandstede, and A. Scheel. Exponential dichotomies for solitary wave solutions of semilinear elliptic equations on infinite cylinders. *J. Diff. Eqns.* **140** (1997) 266–308.
- [27] J.D.M. Rademacher, B. Sandstede and A. Scheel. Computing absolute and essential spectra using continuation. Preprint, 2005.
- [28] B. Sandstede. Stability of multiple-pulse solutions. *Trans. Amer. Math. Soc.* **350** (1998) 429–472.
- [29] B. Sandstede and A. Scheel. Essential instability of pulses and bifurcations to modulated travelling waves. *Proc. Roy. Soc. Edinburgh A* **129** (1999) 1263–1290.
- [30] B. Sandstede and A. Scheel. Absolute and convective instabilities of waves on unbounded and large bounded domains. *Physica D* **145** (2000) 233–277.
- [31] B. Sandstede and A. Scheel. Absolute versus convective instability of spiral waves. *Phys. Rev. E* **62** (2000) 7708–7714.
- [32] B. Sandstede and A. Scheel. Essential instabilities of fronts: Bifurcation and bifurcation failure. *Dynamical Systems* **16** (2001) 1–28.
- [33] B. Sandstede and A. Scheel. On the structure of spectra of modulated travelling waves. *Math. Nachr.* **232** (2001) 39–93.
- [34] B. Sandstede and A. Scheel. Defects in oscillatory media: toward a classification. *SIAM J. Appl. Dyn. Syst.* **3** (2004) 1–68.
- [35] B. Sandstede and A. Scheel. Evans function and blow-up methods in critical eigenvalue problems. *Discr. Contin. Dyn. Syst.* **10** (2004) 941–964.

- [36] B. Sandstede and A. Scheel. Basin boundaries and bifurcations near convective instabilities: A case study. *J. Diff. Eqns.* **208** (2005) 176–193.
- [37] B. Sandstede and A. Scheel. Curvature effects on spiral spectra: Generation of point eigenvalues near branch points. *Phys. Rev. E* **73** (2006) 016217.
- [38] B. Sandstede and A. Scheel. Dynamics of spiral waves. In preparation.
- [39] B. Sandstede, A. Scheel and C. Wulff. Dynamics of spiral waves on unbounded domains using center-manifold reduction. *J. Differ. Eqns.* **141** (1997) 122–149.
- [40] B. Sandstede, A. Scheel and C. Wulff. Bifurcations and dynamics of spiral waves. *J. Nonl. Sci.* **9** (1999) 439–478.
- [41] P. Wheeler and D. Barkley. Computation of spiral spectra. *SIAM J. Appl. Dyn. Syst.* **5** (2006) 157–177.
- [42] A. Winfree. Varieties of spiral wave behavior: an experimentalist’s approach to the theory of excitable media. *Chaos* **1** (1991) 303–334.
- [43] M. Yoneyama, A. Fujii and S. Maeda. Wavelength-doubled spiral fragments in photosensitive monolayers. *J. Amer. Chem. Soc.* **117** (1995) 8188–9191.
- [44] M. Zhan and R. Kapral. Model for line defects in complex-oscillatory spiral waves. *Phys Rev. E* **72** (2005) 046221.
- [45] L.Q. Zhou and Q. Ouyang. Spiral instabilities in a reaction-diffusion system. *J. Phys. Chem. A* **105** (2001) 112–118.